Use of Statistical Mechanics Methods to Assess the Effects of Localized Muscle Fatigue on Stability during Upright Stance

HongBo Zhang

Thesis submitted to the Faculty of the Virginia Polytechnic Institute and State University in partial fulfillment of the requirements for the degree of

Master of Science
In
Industrial and Systems Engineering
Under
Human Factors and Ergonomics Option

Dr. Maury A. Nussbaum, Chair

Dr. Kari L. Babski-Reeves

Dr. Michael L. Madigan

Defense Date: December 11, 2006

Blacksburg, VA

Keywords: Balance, Proprioception, Postural Control, Stabilogram Diffusion Algorithm, Hurst Exponent, Wavelet Transform, Localized Muscle Fatigue

Use of Statistical Mechanics Methods to Assess the Effects of Localized Muscle Fatigue on Stability during Upright Stance

Hongbo Zhang

Committee Chair: Dr. Maury A. Nussbaum, Industrial and Systems Engineering

Summary

Human postural control is a complex process, but that is critical to understand in order to reduce the prevalence of occupational falls. Localized muscle fatigue (LMF), altered sensory input, and inter-individual differences (e.g. age and gender) have been shown to influence postural control, and numerous methods have been developed in order to quantify such effects. Recently, methods based on statistical mechanics have become popular, and when applied to center of pressure (COP) data, appear to provide new information regarding the postural control system. This study addresses in particular the stabilogram diffusion and Hurst exponent methods. An existing dataset was employed, in which sway during quiet stance was measured under different visual and surface compliance conditions, among both genders and different age groups, as well as before and after induction of localized muscle fatigue at the ankle, knee, torso, and shoulder.

The stabilogram diffusion method determines both short-term and long-term diffusion coefficients, which correspond to open- and closed-loop control of posture, respectively. To do so, a 'critical point' (or critical time interval) needs to be determined to distinguish between the two diffusion regions. Several limitations are inherent in existing methods to determine this critical point. To address this, a new algorithm was developed, based on a wavelet

transform of COP data. The new algorithm is able to detect local maxima over specified frequency bands within COP data; therefore it can identify postural control mechanisms correspondent to those frequency bands.

Results showed that older adults had smaller critical time intervals, and indicating that sway control of older adults was essentially different from young adults. Diffusion coefficients show that among young adults, torso LMF significantly compromised sway stability. In contrast, older adults appeared more resistance to LMF. Similar to earlier work, vision was found to play a crucial role in maintaining sway stability, and that stability was worse under eyes-closed (EC) than eyes-opened (EO) conditions. It was also found that the short-term Hurst exponent was not successful at detecting the effects of LMF on sway stability, likely because of a small sample size. The new critical point identification algorithm was verified to have better sensitivity and reliability than the traditional approach. The new algorithm can be used in future work to aid in the assessment of postural control and the mechanisms underlying this control.

Table of Contents

List of Figures

List of Tables

Chapter 1 Introduction

1.1 Background

Occupational falls made up 13 percent of U.S. workplace fatalities in 2002 (US Department of Labor, 2002). Approximately 75% of deaths due to falls in the United States occur in the 14% of the population that is 65 years of age and older (e.g., Riddle and Stratford, 1990). Localized muscle fatigue (LMF) has been regarded as a potential factor increasing the risk of falls (Pfeifer, et al., 2001). For example, Phillip and Hertel (2004 a, b) showed that hip and knee localized muscle fatigue can disrupt frontal plane upright stance stability. Pierre-Jean et al. (1997) indicated that the knee proprioception was reduced after heavy exercise bouts. In the following, we will discuss the role of LMF in upright stance.

LMF has been defined as an exercise-induced loss of the capacity of a muscle to produce physical effort. LMF compromises muscle mechanical performance, making the muscle weaker, slower and leading to loss of exertion forces. In addition proprioception (ability to sense and reposition joint orientation) is adversely affected by LMF (e.g., Joseph et al., 1999; Nicolas et al., 2002; Simo et al., 1999), likely due to a disruption of somatosensory feedback. LMF can occur in two ways: either through proximal motor neurons, or through the distal motor neurons, motor endplates, peripheral nerves and muscle fibers.

It has been widely accepted that input from sensory systems are essentially related to posture stability (e.g., Pierre-Jean et al., 1997, Johansson and Magnusson, 1991, Dietz, 1992). Control of posture during upright stance is achieved by integration of three

sensory inputs (proprioception, vision, and vestibular system), and generation of appropriate motor (muscle) output. In our research, healthy vestibular participants were involved, therefore only the influences on postural control of somatosensation, vision, age, and gender are discussed in detail.

Firstly, proprioception is the sense of the relative position of neighbouring parts of the body. It was shown that, for instance, ankle proprioception is critical for establishing quasi-static sway equilibrium conditions (Massion, 1994). During LMF, the energy substrates around the joint and muscles are depleted, forcing the proprioceptors (e.g., golgi tendon organ and muscle spindles) to work in an insufficient energy environment. As a result, proprioceptors are not capable of reporting accurate limb positions to the brain. Miura et al. (2004) specified that general loads (for example, running on the treadmill) affect central processing of proprioceptive signals, and thereafter lead to a decreased position reproduction ability. This indicates an apparent relationship between LMF and inhibited performance of central processing of signals from proprioceptors. Based on these results, proprioception was regarded as an essential issue to be evaluated in our study.

Secondly, vision also plays a critical role in maintaining the upright stance posture stability. Without visual input, people exhibit higher sway magnitudes (e.g., Loughlin et al., 1996). The interaction between LMF and vision on postural control and postural stability has been investigated by Caron (2004), who reported that LMF increased sway much more in eyes-opened than eyes-closed conditions.

In addition, Kent-Braun et al. (2002) suggested that upright stance stability is highly correlated with age and gender. The correlation between LMF and age and gender is complicated and poorly known. It has been widely accepted that elderly individuals suffered from a loss of muscle mass and functions (e.g., Deschenes, 2004), which might leads to the different sway responses following LMF. However, more detailed correlation between LMF and age needs to be investigated in our study.

1.2 Research Scope

Theoretically, sway can be simplified to a single link inverted pendulum model (e.g., Johansson et al., 1988) or a multiple link inverted pendulum model (e.g., Kuo, 1995). By establishing the single/multiple rigid body models, sway position, velocity and acceleration reflecting upright stance stability can be assessed. Currently, it is still difficult to build a fully physiologically-motivated inverted pendulum model due to the difficulties involved in constructing muscle models. On the contrary, we investigated upright stance stability here using center of pressure (COP) data and several signal processing techniques. It was expected that by adequately processing the COP data, the upright stance control mechanism can be identified.

As a result, the scope of this research was to assess the effects of LMF on upright stance stability and control by developing suitable methods for processing COP data. After reviewing existing methods frequently used to assess sway (e.g., Prieto, 1996; Bagchee et al., 1998), statistical mechanics methods were chosen evaluate sway stability. The principal advantages of such statistical mechanics methods are: (1) the availability of the time domain information yields improved understanding of the physiology involved in

sway control and the effects of LMF; and (2) compared with other time domain and frequency domain measures, they are more robust. In this research, the wavelet transform method was applied along with existing statistical mechanics methods: stabilogram diffusion algorithm (so-called diffusion algorithm) and Hurst exponent algorithm.

1.3 Research Objective

This research aimed at understanding the changes of upright stance stability and control resulting from various independent variables using two statistical mechanics methods. The first method was an enhanced version of the existing stabilogram diffusion algorithm, while the second was an existing Hurst exponent method. These two methods have been widely used to process pseudo-random data (e.g., COP data), however there are several drawbacks associated with these two methods. The details regarding these drawbacks will be given in the methodology part. In order to overcome these drawbacks, a method was developed using the local maximum power spectrum derived from a wavelet of COP data. This newly established method is capable of more precisely calculating an essential parameter, i.e. the critical time interval that distinguishes open-loop and closed-loop control of postural sway. The specific research objective was to integrate the new critical time interval into the diffusion algorithm and the Hurst exponent method, and subsequently evaluate the effects of LMF, vision, support surface compliance, age and gender on postural control during upright stance.

1.4 Thesis Organization

This thesis consists of six chapters. The first chapter presented an introduction to this research. The second chapter reviews the literature regarding processing of COP data and introduces the motivation for new methodologies. The third chapter gives the methodologies used in this research, while the fourth chapter shows the research results. The fifth chapter discusses the results and their implications. The sixth chapter gives the conclusions and suggests future research directions.

Chapter 2 Literature Review and Motivation for New Methodologies

This section reviews existing methods used to process COP data for assessing stability of upright stance. The COP measures are primarily classified into two groups: traditional measures and modern measures. Traditional measures include time domain "distance" measures, time domain "area" measures, time domain "hybrid" measures, and frequency domain measures. Modern measures are derived from statistical mechanics, specifically the Hurst exponent and diffusion methods. The classification of traditional measures is adapted from the review given by Prieto et al. (1996).

2.1 Time Domain Measures

Time domain "distance" measures aim at measuring the distance of the stabilogram, and include mean distance, root mean square distance, mean velocity methods. Time domain "area" measures include 95% confidence area and the sway area methods. The 95% confidence circle area measure defines a circle with a radius equal to the one-sided 95% confidence limit of time series data. The sway area measure was created to calculate the areas enclosed by the COP path per unit of time. As an example, ellipse area method considers the product of the long axis and the short axis of the stabilogram. Hertel & Olmsted-Kramer (2006) presented the time-to-boundary measure (TTB), which defined the time for the center of pressure to move to the foot boundary. The time for sway moving to one foot boundary reflects upright stance stability.

2.2 Frequency Domain Measures

Frequency domain methods assess upright stance stability primarily with the power spectrum. Usually, the frequency band of 0.15-5.0 Hz is of interest when analyzing COP data (Prieto et al. 1996). The mean power frequency (MPF) is the ratio between the weighted products of frequency, and the power in each frequency component and the total power. MPF has been used by Hasan et al. (1996) to assess the difference between the COP and COG power spectrum. Another often used frequency domain method is the 95% power frequency, defined as the frequency below which 95% of total power of COP spectra is found.

2.3 Interpretation of Time and Frequency Domain Measures

Computationally, all of these measures are easy to be implemented. Physically, they are straightforward for describing sway motion, and have been widely used to assess upright stance stability. However, there are two principal drawbacks to traditional time and frequency domain measures. Firstly, COP data may be non-stationary, therefore, mean and standard deviations applied in the time domain are not appropriate due to the existence of long term dependencies in the COP data. Secondly, the mean power frequency and other traditional frequency measures are not able to assess time dependent changes in the power spectrum, and thus cannot be used to investigate time dependent changes in the mechanisms of upright stance control.

2.4 Statistical Mechanics Measures to Assess the Stability of Upright Stance

2.4.1 Stabilogram-diffusion Algorithm

Collins and DeLuca (1993, 1994, 1995a, 1995b, 1995c) indicated that COP data recorded during quiet upright stance can be interpreted as a correlated random walk with noise, which means that the COP motion is driven by both deterministic and stochastic forces. The diffusion equation can be written in terms of mean square displacements and time intervals, denoted as

$$\left\langle \Delta x^2 \right\rangle = 2D\Delta t$$

where D is the diffusion coefficient. It implies that there is a linear relationship between mean square displacements and the time interval. Fraction Brownian motion can also be generalized to the following scaling law

$$\left\langle \Delta x^2 \right\rangle = \Delta t^{2H}$$

where the scaling exponent H $\left(0 < H < 1\right)$ is a real number. If H=1/2, the motion is a classical Brownian motion. If H<1/2, previous motions are negatively correlated with future motions. In contrast, if H>1/2, previous motions are positively correlated with future motions.

Mean square displacements are calculated by:

$$\left\langle \Delta r^2 \right\rangle_{\Delta t} = \frac{\sum_{i=1}^{N-m} \left(\Delta r_i\right)^2}{N - m}$$

where Δr_i is the displacement from (x_i, y_i) to (x_{i+m}, y_{i+m}), m is the m^{th} step, and N is the total number of steps. Δr_i is the COP displacement during a Δt time interval, where m points were spanned. Calculating the mean square displacement is quite computationally intensive. An efficient method to calculate the mean square displacement is given in Appendix A. An example stabilogram diffusion plot and log-log stabilogram diffusion plot are shown in Figure 1.

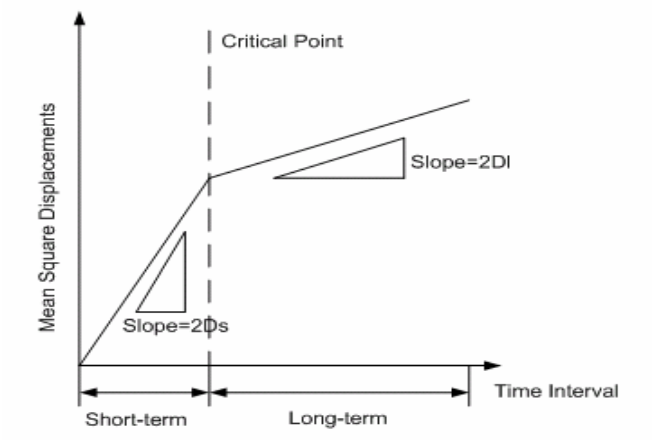

(a)

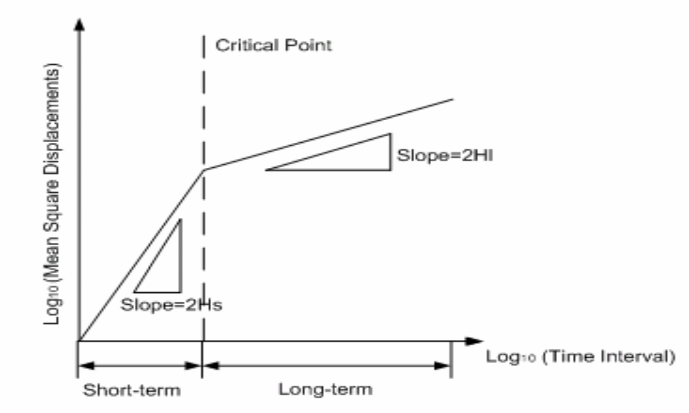

(b)

Figure 1: Stabilogram diffusion plot (a) and log-log stabilogram diffusion (b)

2.4.2 The Procedures for Implementing the Stabilogram Diffusion Algorithm

(1) Calculate the mean square displacement.

(2) Filter the data with respect to both medio-lateral and antero-posterior directions with Butterworth second order filtering method, cutoff frequency 5.0 Hz (99% of COP energy concentrated below 5.0 Hz) .

(3) Determine the following four points used to fit the short-term and long-term diffusion regression lines,

(a) The critical point

(b) The last point of the short-term diffusion region

(c) The first point of the long-term diffusion region

(d) The last point of the long-term diffusion region.

(4) Obtain the regression lines for both short-term diffusion coefficients and long-term diffusion coefficients regions.

(5) Derive the short-term and long-term diffusion coefficient D with

$$\mathrm{D} = \frac{\mathrm{Slope}_{\mathrm{Diffusion}}}{2}$$

where D is the diffusion coefficient, and $\mathrm{Slope}_{\mathrm{Diffusion}}$ is the slope of the regression line.

(6) Calculate the scaling exponent H, which is the half slope of Log-Log time interval-mean square displacement plot, with following equations.

$$\left\langle \Delta x^2 \right\rangle = \Delta t^{2H}$$

$$\mathrm{H} = \frac{1}{2}\frac{\mathrm{Log}\left\langle \Delta \mathrm{X}^2 \right\rangle}{\mathrm{Log}\Delta \mathrm{t}}$$

$$\mathrm{H} = \frac{1}{2}\mathrm{Slope}_{\mathrm{Log-Log}}$$

2.4.3 Discussion of Stabilogram Diffusion Algorithms

Linear regression lines can be generated respectively in the short-term and long-term regions of the stabilogram diffusion data. Based on slopes of these linear regression lines, stability of upright stance control can be roughly estimated. Larger slopes of the regression lines imply greater instability of sway, since for a certain time interval, a larger slope corresponds to a larger mean square of displacement or greater sway magnitude. The purpose of dividing the short-term and long-term diffusion regions is to obtain more detail on the mechanisms of upright stance control. It was suggested by Collins and DeLuca (1994) that upright stance control consists of open-loop and closed-loop control, which respectively correspond to posture control strategies in the short-term and long-term diffusion regions. Open-loop control typically indicates that there is no significant sensory feedback (e.g., from proprioceptive, vestibular, or visual afferents) used in stance control. Closed-loop control, in contrast, implies the use of sensory feedback for controlling upright stance. In general, closed-loop control is better than open-loop in maintaining upright stance stability, since more abundant feedback can be utilized by central nervous systems to control sway. The critical point located between the open-loop and closed-loop regions is used to identify the time interval that distinguishes between open-loop and closed-loop control. This critical point is a central focus of the algorithm developed and evaluated in the current research.

Although slopes from diffusion analysis can be used to estimate upright stance stability, they cannot detect nonlinearity (scaling-violation phenomena) of sway. Detecting nonlinear relationships between upright stance sway and the time interval is essential in assessing upright stance stability (Thurner et al., 2000). Without a complete analysis of

nonlinearity, LMF effects on sway will not be able to be fully determined. The newly proposed wavelet transform method has the potential to detect such nonlinearity.

A second drawback is that the critical point (transition between open- and closed-loop control) has been determined without solid physiological support. Heuristic methods are applied to determine the points used for fitting regression lines, therefore precision has not been ensured. This problem is addressed in the current algorithm.

2.4.4 Hurst Exponent Methods

The Hurst exponent has been frequently used to calculate the long-term correlation of time series data. Several investigators (Duarte and Zatsiorsky, 2000; Daniel et al. 2004; Michel and Matt, 2005) have shown that the stability of upright stance can be described by the Hurst exponent. The R/S statistics calculates the cumulative displacements of a random variable $\mathrm{u(i)}$ denoting the i[th] COP data with respect to either ML or AP directions within k steps.

$$\mathrm{y(k)} = \sum_{\mathrm{i=1}}^{\mathrm{k}} \mathrm{u(i)}$$

The fluctuation within k steps then becomes

$$R(t,k) = \max_{0 \le i \le k}\left[y_{t+1} - y_t - \frac{i}{k}\left(y_{t+k} - y_t\right)\right] - \min_{0 \le i \le k}\left[y_{t+1} - y_t - \frac{i}{k}\left(y_{t+k} - y_t\right)\right]$$

The normalized $R(t,k)$ is

$$S(t,k) = \sqrt{k^{-1}\sum_{i=t+1}^{t+k}\left(u_i - \bar{u}_{t,k}\right)^2}$$

Then

$R/S = \frac{R(t,k)}{S(t,k)}$, which is scale-independent.

There is a power law relationship between R/S and k

$$R/S \equiv \left(\frac{k}{2}\right)^{H}$$

$$H = Slope_{Log(R/S)-Log(k/2)}$$

Where H is the slope of linear regression line between log(R/S) and log(k/2). H can be interpreted as the fractal dimension of a univariate time series.

Like diffusion analysis, if H=0.5, the data represent pure Brownian random motion, where correlations are non-existent. If H > 0.5, then there is persistent behavior, which indicates that past displacements determine future displacements. If H < 0.5, then there is anti-persistent behavior, which indicates that future displacement are opposite to past displacements. Procedures for determining the Hurst exponent for COP are shown in Figure 2.

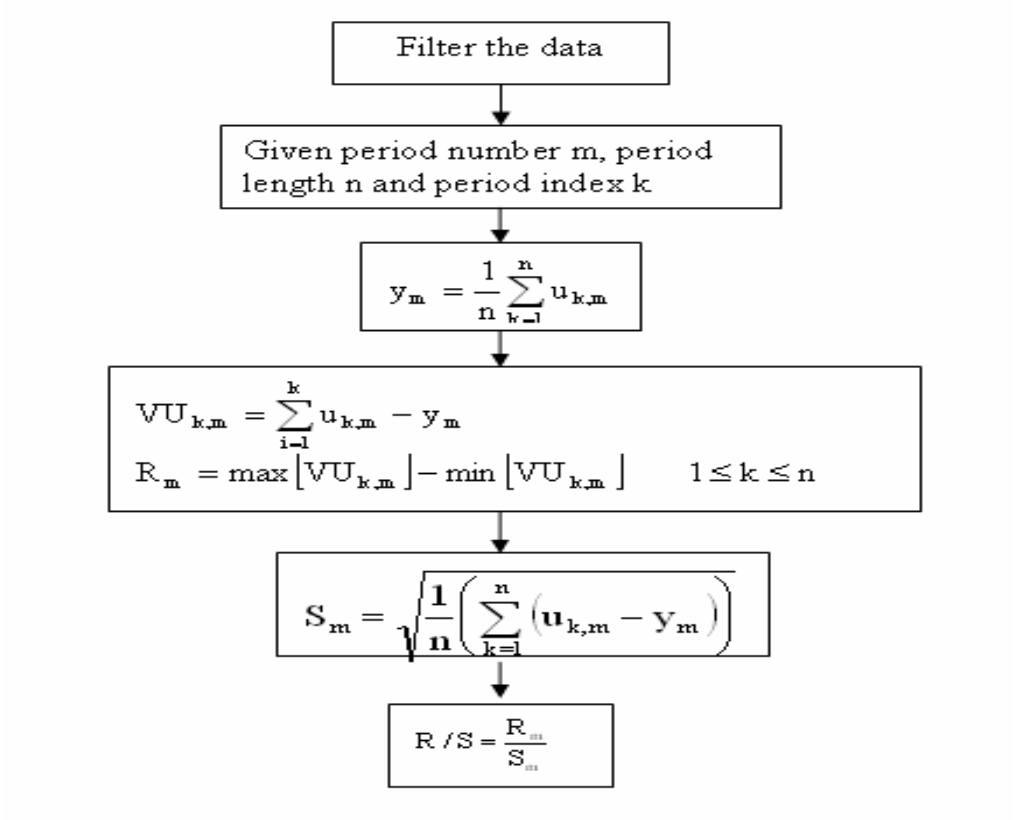

Figure 2: Procedures for calculating the Hurst exponent of COP data

2.4.5 Discussion of Hurst Exponent Algorithm

The Hurst exponent has been shown to give stable results for analysis of time series data by several researchers (e.g., Cajueiro and Tabak, 2004; Couillard and Davison, 2005). The Hurst exponent method is also more robust than traditional time and frequency domain COP analysis methods in assessing sway stability (Doyle et al., 2005). The Hurst exponent also requires low computational complexity, and is therefore an efficient tool to evaluate the stability of upright stance.

The Hurst exponent also has several limitations. Firstly, the amount of data needed to compute Hurst exponent is large (Couillard and Davison, 2005), with previous studies

using 30 minutes. However, in our study, COP data were obtained for 60 seconds, which may be not sufficient to calculate the Hurst exponent. Secondly, the data used to calculate Hurst exponent have to be stationary. Unfortunately, there is still a debate whether upright stance COP data are stationary or non-stationary (Carroll and Freedman, 1993). The most significant drawback of R/S exponent analysis is that the short-range correlations can bias the Hurst exponent and result in a misjudgment that long-term memory exists (Couillard and Davison, 2005).

2.5 Motivation for Proposing the New Method

2.5.1 Drawbacks of the Existing Stabilogram Diffusion Algorithm

Collins and DeLuca (1994) presented a method to calculate the critical time intervals and time intervals used to fit regression lines. In the following, time intervals are simply denoted as points, since they are used to fit regression lines.

(1) The mean square displacemen, known as diffusion data was calculated based on the COP data by the method in appendix A. The second order derivative of the diffusion data (SOD-DD) was computed, and the consecutive operations were executed based on SOD-DD.

(2) The first point for fitting the short-term diffusion coefficient is set to zero.

(3) The second point for fitting the short-term diffusion coefficient is defined as the first maximum of SOD-DD within one second.

(4) The critical point is the first minimum of SOD-DD within 2.5 seconds.

(5) The third point for fitting the long-term diffusion coefficient is defined as the second local maximum of SOD-DD from the critical point.

(6) The fourth point for fitting the long-term diffusion coefficient is defined as the first maximum to the left of the first minimum of SOD-DD going back from 9 seconds.

This method is easy to implement with acceptable efficiency. It was developed based on the following physical motivations.

(1) SOD-DD is proportional to the acceleration of the sway, therefore it can be approximately regarded as the acceleration of the sway. Suppose sway is moving to the positive direction, the local minimum of the acceleration within 2.5 seconds is correspondent to the smallest positive ground reaction force. At this local minimum, sway tends to be back to the equilibrium point by the feedback control, therefore local minimum is the critical time interval.

(2) The first maximum of SOD-DD corresponds to the largest positive ground reaction force. It means negative ground reaction force has not dominated the sway, i.e., the feedback control has not been fully used yet. As a result, this point is the second point used to fit the short-term diffusion regression line indicating the end of open-loop control (the first point is always set to zero).

(3) The third and fourth points correspond to the first and last points used to fit the long-term diffusion regression line. There seems to be no solid physical rationality for determining these two points.

Although (1) and (2) are motivated by posture control strategies, it is somewhat bold to judge that the critical time interval has to occur within 2.5 seconds, and the second point used to fit the short-term regression line has to be within 1 second. According to our knowledge, there are no methods able to avoid using fixed time thresholds to determine

points used to fit these regression lines. This is also one of the major difficulties faced by Collins and DeLuca (1994).

Norris et al., (2005) simplified the regression points and critical points identification process with following procedures:

(1) The short-term diffusion regression lines were continuously fitted on the intervals $\Delta t \in [0.00, 0.10]$, $\Delta t \in [0.00, 0.11]$, ... , $\Delta t \in [0.00, 3.99]$, $\Delta t \in [0.00, 4.00]$. The last point used to fit the short-term regression line corresponds to the time interval with minimum R^2 of these regression lines.

(2) The long-term diffusion regression lines were continuously fitted on the intervals $\Delta t \in [4.00, 10]$, $\Delta t \in [4.01, 10]$, … , $\Delta t \in [9.89, 10]$, $\Delta t \in [9.90, 10]$. The last point used to fit the long-term regression line corresponds to the time interval with minimum R^2 of these regression lines.

(3) The critical point is at the intersection of the short-term regression line and the long-term regression line.

This method is simple and efficient, however there are some drawbacks inherent in this method too. Firstly, the points used to fit the short-term and long-term regression lines were identified through statistical techniques instead of posture control strategies. Secondly, without support from the literature, using 4 seconds as the time interval to distinguish the short-term and long-term regression intervals is questionable. Thirdly, this critical point identification method only has a statistical meaning, and it does not reflect the physiology of upright stance posture control.

2.5.2 How to Improve the Hurst Exponent Method

Duarte and Zatsiorsky (2000) proposed that the time interval for Hurst exponent should be specified up to 30 minutes. In the present sway study, only 60 seconds of COP data were used to calculate the Hurst exponent. During the open-loop control period, sway moves away from the equilibrium point (Lipsitz, 2002), which indicates larger sway motion in the open-loop control period than the closed-loop control period. As a result, the open-loop control Hurst exponent can assess larger sway motions compared with the closed-loop Hurst exponent. Thus, in our study, we focused on calculating the short-term (corresponding to open-loop control) Hurst exponents in the open-loop control time interval. Our purposes were to explore: (1) whether it is possible to obtain reasonable values of the short-term Hurst exponent for short durations of sway data (i.e. is the short-term value obtained from 60 seconds of sway data similar to that obtained in earlier research over 30 minutes?) (2) whether the short-term Hurst exponent quantifies sway stability similar to the open-loop diffusion coefficient.

Chapter 3 Research Methodologies and Preliminary Results

3.1 Acquisition of COP Data

Data obtained from a previous study were employed in the current investigation. In the prior study, sway data during upright stance were obtained under baseline conditions, as well as pre- and post-fatigue.

The baseline contains eyes-opened (EO), eyes-closed (EC), firm and compliant surface conditions. Participants stood upright on a force plate in each combination of the two visual and supporting conditions. Differences in sway stability on firm and complaint surfaces and with eyes-opened and eyes-closed were expected. In addition to vision and surface compliance, gender and age were independent variables in the baseline study. COP data were obtained from a force plate, and body motion captured using an optoelectronic system (the latter not analyzed here).

The ankle, knee, torso and shoulder may play different roles in maintaining upright stance stability. It is thus important to understand potential changes to upright stance control resulting from LMF at these joints. To do so, LMF was induced in each joint separately. Standing sway was recorded before and after LMF, while participants stood on a firm surface with their eyes closed.

3.2 Participants

A total of 32 participants were included in the baseline and LMF sessions. Participants were equally divided between genders and younger and older groups. All participants completed an informed consent procedure approved by the Virginia Tech IRB, and were

screened for current and recent injuries, illness, musculoskeletal disorders and falls. Information on participants is listed in Table 1.

Table 1: Participant Characteristics (n=8 in each group)

	Age(years)	Stature (cm)	Body Mass (kg)
Males(Young)	20.3(1.4)	176.0(4.6)	72.1(12.3)
Females(Young)	21.4(1.8)	166.6(5.7)	62.7(6.7)
Males(Old)	65.6(3.5)	175.5(12.4)	88.9(7.6)
Females(Old)	60.8(6.0)	160.2(14.8)	66.2(7.1)

3.3 Procedures

The experiment consisted of three phases, the baseline phase, fatigue inducing phase and post-fatigue data collection phase. During the baseline phase, participants were instructed to stand on the force plate (AMTI OR6-7-1000, Massachusetts, USA), and COP was recorded. In the second phase, LMF was induced at a specific joint through repetitive isotonic exertions, using a commercial dynamometer (Biodex 3 Pro, Biodex Medical Systems Inc., New York, USA). Details on fatigue induction are provided below.

During the second phase, each participant was involved in five sub-sessions, consisting of one practice session and four consecutive sessions as following: (1) A warm up session consisting of 2 sets of 10 repetitions each, including calf raises for the ankle LMF, squats for the knee LMF, stoops for the low back LMF and arm raises for the shoulder LMF. (2) Isokinetic maximum voluntary contractions (MVC) session, five replications, at a speed of 60°/sec, with at least one minute interval were conducted to determine the load used for exercises. Participants were required to perform exertions through a set range of

motion of 45°, from 15° dorsiflexion to 30° plantar-flexion for the ankle, from 10° flexion to 35° extension for the knee, from 45° flexion to the upright position for the torso, and from 0° to 45° flexion for the shoulder. (3) Sham exercise session, sham was conducted passively in 10 minutes with 12 repetitions/min. The passive motion range was same as the motion range used for MVC. One more MVC was performed after sham. Immediately after MVC (within 45s), participants were asked to step on the force plate. (4) Finally, participants were performed sub-maximal (60% MVC) isotonic exercise at 12 repetitions/min to induce fatigue in the ankle plantar flexors, knee extensors, torso extensors and shoulder flexors (each joint tested in separate experimental sessions). The range of motion for fatiguing exercises was same as that used for MVC. Participants were required to start the exertion at sound of a computer-generated first beep and try to reach the end range of motion by a second beep. Fatiguing exercise was continued until participants were not able to finish three consecutive exercises. Following the fatigue induction phase, the post-fatigue sway data were obtained.

3.4 COP Data

Because the aim of this research was to analyze COP data and thereafter assess the upright stance stability, COP data need to be clarified. The instructions used to measure the COP data were to stand as quiet as possible, with feet together, head upright and eyes-closed. The COP data consist of 15 trials. The first to the third trials were measured before localized muscle fatigue, and the fourth trial was measured under the sham condition. The fifth to fifteenth trials were measured following LMF. The COP data were captured with a sampling frequency of 100Hz for 75 seconds. The first 10 and the

last 5 seconds of data were eliminated to avoid translational effects. As a result, only the remaining 60 seconds COP data were used to evaluate upright stance stability.

3.5 Identifying the Critical Point Using Wavelet Transform Analysis

3.5.1 Locating the Critical Point

When upright stance control is changed from open-loop to closed-loop control, energy consumption should first reach and then leave a local maximum. A local maximum in energy consumption should in turn correspond to a local maximum in the COP power spectrum. Reasons for the critical point being located at the local maximum of COP power spectrum are the following:

(1) The critical point is defined as the time interval, beyond which sway is under the closed-loop (feedback) control. When upright stance is under open-loop control, sway moves toward a certain direction and reaches a local maximum. Central balance correction commands from closed-loop control systems driven the sway to move away from the local maximum and back to the equilibrium position along the opposite direction. Therefore, the critical point corresponds to the time when energy consumption is at a local maximum. Although this idea is similar to the idea underlying the traditional method proposed by Collins and DeLuca (1994), there is a significant difference between the new and traditional methods. In the new method, the local maximum is located in the frequency domain, as opposed to the time domain in the traditional method.

(2) If the critical point does not correspond to a local maximum (in the absolute value sense), apparently it means that sway has been controlled indicating the feedback control has already been used. As a result, non-local maximum points are not

critical points. Figure 3 illustrated an example local maximum where feedback control occurred.

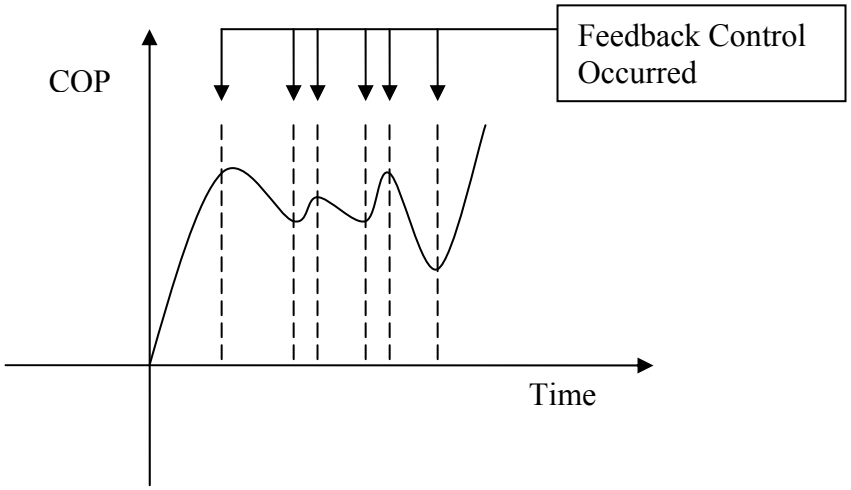

Figure 3: Feedback Control and the Local Maximum of COP

From the arguments given above, it can be concluded that the critical point corresponds to the time interval when the power spectrum is at a local maximum. Mathematically, the local maximum points are also denoted as the singularity points. Mallat & Hwang (1991) indicated that local maximum modulus wavelet transform is particularly well adapted to estimate the local regularity of functions. They proved that all singularities (local maximum) of arbitrary functions can be detected by the local maximum modulus wavelet transform method. Therefore in our research, the local maximum modulus wavelet transform method was adopted to detect the local maxima. The local maximum power spectrum wavelet transform method employed in this research is similar to the local maximum modulus wavelet transform method. The only difference between the new and traditional methods is that the power spectrum instead of the modulus was applied in our study, where the power spectrum is equal to the square of the modulus. The reason to

employ the power spectrum instead of the modulus is because the power spectrum represents the energy in sway.

3.5.2 Wavelet Function and Frequency Bands

The wavelet transform method is one of the most powerful mathematical tools for signal analysis (e.g., Muzzy et al., 1993; Redfern et al., 1995; Jaffard,1997; Ivanov et al., 1999 ; Plamen et al., 1999). It is particularly suitable for analyzing non-stationary signals. The wavelet transform method also has the advantage of analyzing signals in a multi-scale manner by varying the scale coefficient (representing frequency).

The wavelet transform formula is

$$WT(a,b) = |a|^{-1/2} \int f(t)\varphi\left(\frac{t-b}{a}\right)dt$$

where b is the translation parameter and a is the scale (frequency), and $WT(a,b)$ is the wavelet coefficient.

The power spectrum $\mathrm{PS(a,b)}$ is defined as

$$\mathrm{PS(a,b)} = \left|\mathrm{WT(a,b)}\right|^2$$

Wavelet function $\varphi(x)$ should satisfy the following constraints (e.g., Muzzy et al., 1993):
(1) It should have zero mean to achieve invertibility. φ should be orthogonal to the low order polynomials. This property is also known as the orthogonal requirement.

$$\int_0^{+\infty} t^m \varphi(t)dt = 0 \qquad \forall m, 0 \le m < N$$

$\varphi(t)$ decays rapidly to zero when $|t| \to \infty$.

(2) The selected wavelet function should be able to decrease low frequency distortion. Low frequency distortion is a drawback of the wavelet transform, which indicates the transform introduced noise to the wavelet coefficients in low frequency bands.

There are several wavelet functions satisfying orthogonal requirements, for instance Haar, derivate of Gaussian function, Coiflets, etc. Haar and Coiflets wavelet functions were found to be the most effective at reducing low frequency distortion in our COP data. These wavelet functions are symmetric, and as such they are suitable for representation and approximation of signal details. More theoretical proofs for the efficiency of Coiflets wavelet functions can be found in the work of Wei & Bovik (1998) and Tian & Wells (1995). As a result, either Haar or Coiflets wavelet function can be used to calculate the COP power spectrum.

It has been shown (Ferdjallah et al., 1999) that 90% of sway energy is distributed in frequencies below 2 Hz. Other research (e.g., Schmuckler, 1997; Loughlin et al., 1996) indicated that the principal energy of COP should be distributed in the range of 0.1-0.5 Hz. Based on our wavelet analysis, it was shown that most of sway energy concentrated within 0-0.5 Hz. In Figure 4, it is apparent that the principal power spectrum energy is located within frequency bands 0.0-0.5 Hz. Since the frequency bands of principal energy (90%) are below 2.0 Hz, then roughly the frequency band [0.1, 2.0] Hz can be used for the power spectrum wavelet transform analysis. For wavelet function $\varphi(x)$, scale a determines the frequency and b determines the translation. Thus we choose the appropriate scale parameter a, enforcing the frequency of wavelet transformation to the

range of 0.1-2.0 Hz. A sample power spectrum of COP data in AP direction was shown in Figure 4.

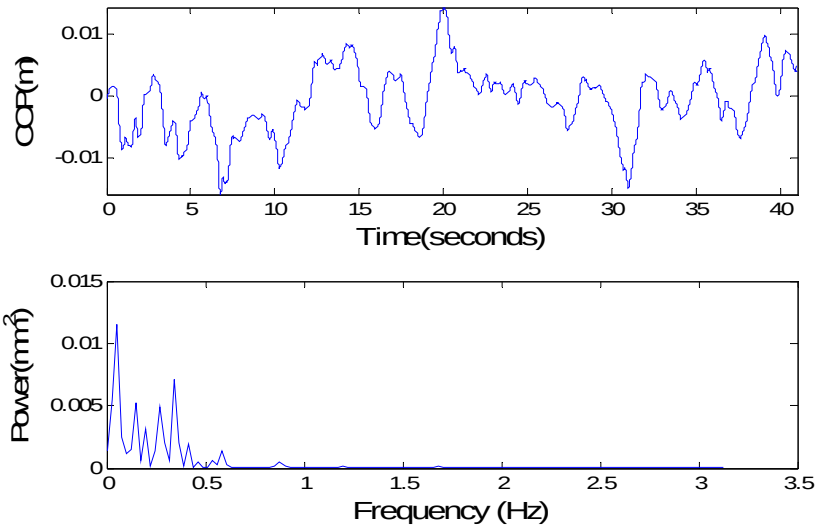

Figure 4: Sample power spectrum of COP data (AP direction)

Considering the relation between the scale and frequency

$$F_a = \frac{F_C}{a \cdot P}$$

F_C: The center frequency

F_a: The frequency for scale a

P: The sampling period (Here 0.01 sec.)

For Coif1 wavelet function, the center frequency is 0.8 Hz, therefore the scale a is

$$a = \frac{F_C}{F_a \cdot P} = \frac{0.8}{0.01 \times [0.1, 2]}$$

$$a = [40 - 800]$$

In Figure 5, the center frequency of the Coif1 wavelet function was given.

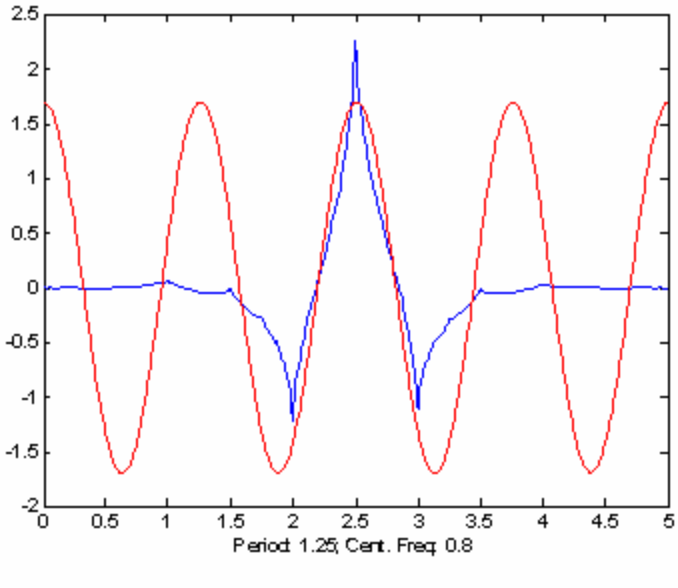

Figure 5: Center frequency of the Coif1 wavelet function, where a cosine curve was used to fit the period of coif1 wavelet function (its shape similar to a hat).

It is evident that the scale a should be in the range of [40-800]. If we take the base-2 logarithm value of the scale a and denote it as a new scale s, we then have

s =Log2 (a)
s =Log2 ([40-800])
s=[5.3,9.6]

Translation parameter b was forced to be zero. The higher frequency bands contain a small amount of energy. They are also possibly contaminated by noise. Although the lower frequency contains the most part of energy, it is usually hard to detect the instantaneous change of COP signals in lower frequencies. Therefore, there is a balance achieved in frequency selection, i.e. choosing the frequency around 0.1 Hz or around 2.0 Hz for the power spectrum analysis.

Ferdjallah et al. (1999), Schmuckler (1997), and Loughlin et al. (1996) suggested that frequency bands around 0.5 Hz are appropriate to be chosen for COP time-frequency analysis. Diener et al. (1984) and Gagery et al. (1985) have stated that visual system primarily dominates frequency bands below 0.5 Hz in maintaining the stability of upright stance, however this result is too rough to be directly adopted as the frequency bands for our study. It was reported (Thurner et al., 2000) that the visual system is linked to frequency bands in the range of 0-0.1 Hz, which dominates the upright stance posture. Vestibular stress and disturbance dominate frequencies in the range of 0.1-0.5 Hz. Somatosensory activity is associated with the frequency bands in the range of 0.5-1.0 Hz. Central nervous system control is usually related to frequencies of 1.0 Hz or higher. Dietz et al. (1980) found that ankle proprioception reflexes were the principal contributor to frequencies of 4-5 Hz.

In our experiment, except for some baseline conditions, all the upright stance trials are the under eyes-closed visual condition, therefore visual contributions to upright stance control can be excluded. As a result, disturbances to somatosensory acuity are expected to be the most dominant factor for upright stance control. In addition, only healthy vestibular function participants were involved in our study. Furthermore, according to a study of ankle dorsiflexor muscle fatigue (e.g., Kent-braun et al., 2002), it was reported that LMF did not compromise the central activation ratio in any groups of participants indicating the central nervous system was not significantly inhibited due to LMF. Therefore, somatosensory input was treated as the most important factor affecting upright stance stability. Further, the frequencies of 0.5-1.0 Hz were considered to be principally

reflecting postural control, and corresponding to the use of proprioceptive input. As a result, the lower and upper bounds of scale s were chosen as 6.5 and 8, respectively. This scale range corresponds to the frequency bands in the range of [0.44, 0.88] Hz. After determining scale s, translation b, and the wavelet function, the power spectrum can be calculated, an example of which is shown in Figure 6. Computational flow of wavelet transform is shown in Figure 7.

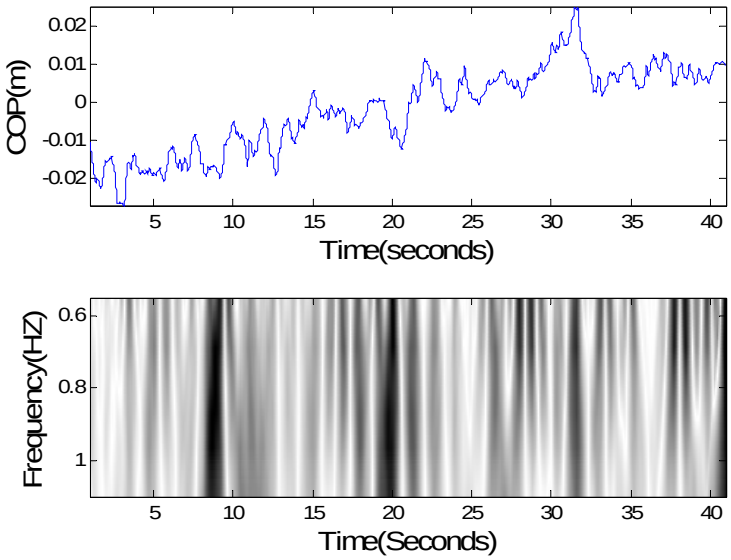

Figure 6: Sample wavelet power spectrum of COP data (ML direction). Darker and lighter areas represent larger positive and negative power spectrum values, respectively.

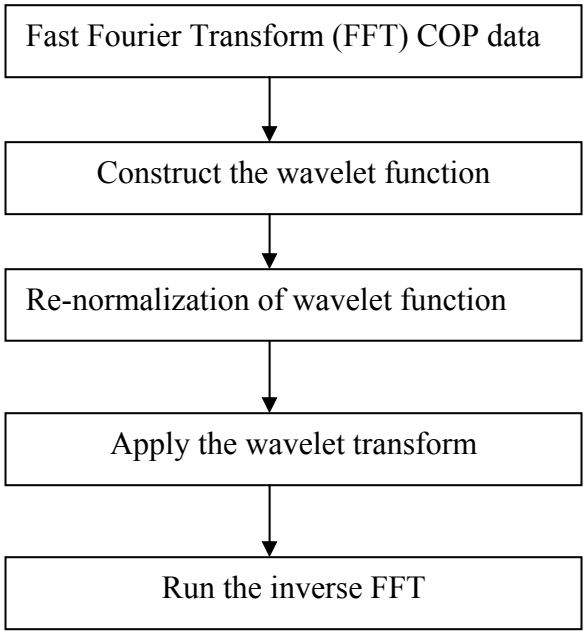

Figure 7: Computational flow of wavelet transform

3.6 Identifying the Critical Time Interval

Humans are capable of changing their control strategies from open-loop control to closed-loop control with visual, vestibular and somatosensory feedbacks. When the feedback control mechanism has been used, sway tends to move away from a local maximum and back to the equilibrium position. The critical point occurs at scale s and time t, where the power spectrum is at the local maximum. It is simply the local maximum of the power spectrum wavelet transform method (LMPS). Mathematically, it is defined as:

$$PS(s, x) < PS(s, x_0)$$

where x is either the left or right neighborhood of x_0, $x \in R$, and s is scale.

There are numerous local maximum points within specific frequency bands, which indicates that feedback control has been started at time t and scale s. Upright stance control corresponds to the frequency bands rather than a single frequency. Therefore, identification of local maximum lines (maxima across the frequency range) was required. A local maximum line L_t was defined as the line consisting of the local maxima at time t across frequency bands from a to b. Mathematically, it can be described as:

$$L_t \overset{d}{=} \{PS(s,t), s = a \cdots b\}$$

For COP data, there is perhaps no such perfect line L_t at time t in the range of scale [a,b]. In our study, the local maximum lines were identified in the frequency bands [a=0.44, b=0.88] Hz, as these frequency bands are associated with the proprioception control as argued above. It is necessary to search for the local maximum around time t within a $2\Delta t$ interval denoted by [t- Δt , t+ Δt]. If the local maximum line L_t can be identified within the time interval [t- Δt , t+ Δt], it is concluded that feedback control has been used at time t. In practice, the time interval Δt used to search for the local maximum line depends on the specific data. For example, when processing the young participant COP data, in order to identify suitable quantity of local maxima, the searching time interval Δt was selected as 0.21 seconds, which was obtained by gradually increasing the Δt value from a very small number (e.g., 0.05 second) until obtaining the suitable quantity of local maxima. Use of Δt bigger than 0.21 second may result in too few local maxima for some sensory inputs (e.g., visual and support compliance conditions). On the contrary, Δt smaller than 0.21 second may result in too many local maxima for some sensory inputs. Vigorous

methods for determining Δt may involve confirming the time delay in the theoretical feedback control.

There are numerous such local maximum lines. Also, there are series of intervals $\{\Delta L_{t1}, \Delta L_{t2}, \ldots, \Delta L_{tn}\}$, which correspond to the intervals between the local maximum lines. Mathematically, this was defined as:

$$\Delta L_{ti} = t_{i+1} - t_{i-1}$$

Physically, the interval between two local maximum lines is the period where there is not substantial control of upright stance. This also suggests that there was no substantial feedback control (e.g., proprioception) in these intervals, and that substantial feedback control only takes place at the boundaries of these intervals.

The critical time interval corresponds to the mean across all identified intervals. The time interval Δt used to search for the local maximum line, the local maximum lines L_t, and the local maximum line interval ΔL_t are illustrated in Figure 8. In this figure, the first local maximum line arises at time t1 around 0.5 second (50 sampling points). It corresponds to the time when upright stance control (e.g., proprioception) was active. It is also evident that at time t2 (1.2 seconds, 120 sampling points) the proprioceptive control mechanism was used again. In the time interval $\Delta t3$, ranging from 1.9 to 2.5 seconds, proprioceptive control was used in a sequence but not simultaneously. The local

maximum power spectrum wavelet transform was executed according to the steps shown in Figure 8. The algorithm for identifying the critical time interval is shown in Figure 9.

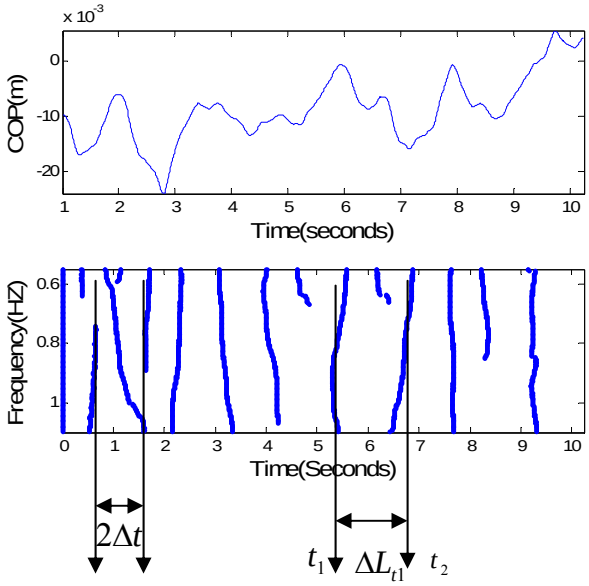

Figure 8: Local Maximum lines and local maximum line intervals, where ΔL_{t1} is the local maximum line interval between time t_1 and t_2, and $2\Delta t$ is the length of the interval used to search for the local maximum line.

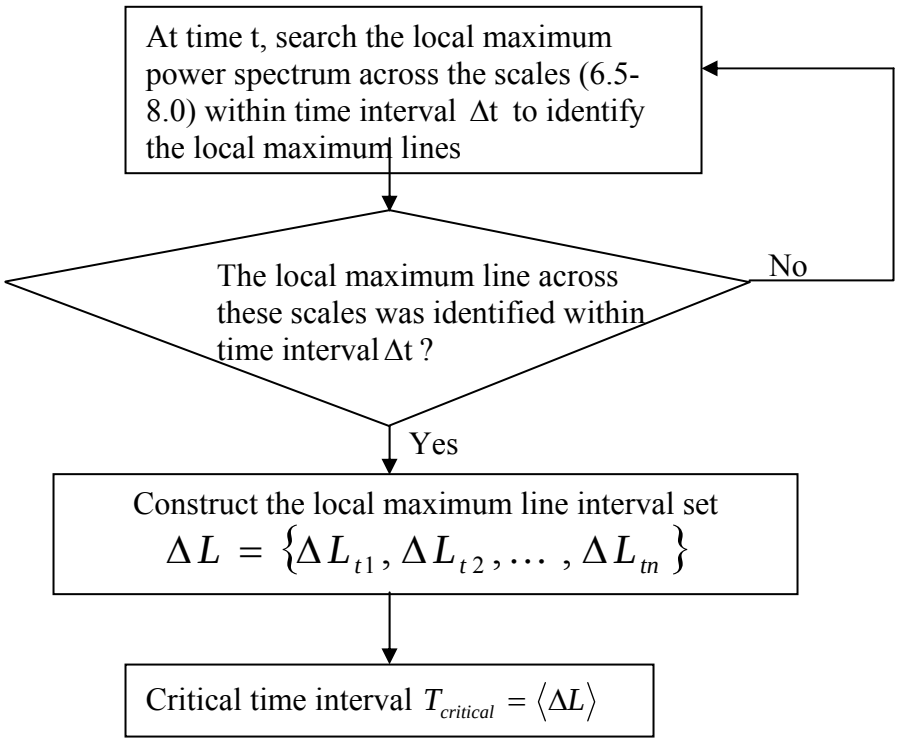

Figure 9: Algorithm for identification of the critical time interval

The mean of the local maximum line intervals is the critical time interval. Besides the critical time interval, the time intervals used to fit regression lines from the diffusion data also need to be determined. In total, two regression lines need to be fitted, respectively to the short-term and long-term regions. The first time interval used to fit the short-term regression line is zero, and the second time interval used to fit the short- term regression line is the lower bound of local maximum line interval set $\{\Delta L_{t1}, \Delta L_{t2}, \ldots, \Delta L_{tn}\}$, denoted as $\underline{\Delta L}$. The first time interval used to fit the long-term regression line is the critical time interval, and the second time interval used to fit the long-term regression line is the upper bound of the local maximum line interval set $\{\Delta L_{t1}, \Delta L_{t2}, \ldots, \Delta L_{tn}\}$ denoted as $\overline{\Delta L}$. It is worth mentioning that the traditional algorithm used a certain time interval after the critical time interval as the first time interval to fit the long-term regression line. In

practice, our study showed that there is not much difference between the critical time interval and the first time interval used to fit the long-term regression line, therefore the first time interval used to fit the long-term regression line can be replaced by the critical time interval.

3.7 Data Analysis Plan

3.7.1 Diffusion Coefficients and Critical Time Interval Analysis Plan

Both young and older participants COP data were processed with the new stabilogram diffusion algorithm, which yielded the short-term diffusion coefficient, long-term diffusion coefficient, and the critical time interval. The scaling coefficient H was also obtained, but its accuracy has not been widely proved. As a result, we focused here on investigating the diffusion coefficients and the critical time interval. Open-loop Hurst exponent H was also calculated with the young participant data. From the experimental (LMF) data, only the pre-fatigue and immediate post-fatigue data were analyzed.
The diffusion coefficient and critical time interval used for statistical analysis are the mean value of three trials before the localized muscle fatigue and the mean value of three trials immediate following the localized muscle fatigue. In this report, without additional notice, p-values to determine statistical significance were 0.05. The main effects of gender, fatigue, joint and age were determined with ANOVA. Interactions effects between the gender, fatigue and joint were not considered. JMP software was used for statistical analysis.

3.7.2 Critical Time Interval Sensitivity Analysis Plan

Sensitivity is an important measure to evaluate the robustness of the new critical time interval searching algorithm. In the traditional diffusion algorithm, the critical time interval was obtained with the following procedure: the critical point is the first minimum of second order derivate of diffusion data within searching interval (SINT) 2.5 seconds. In order to verify the sensitivity of the traditional diffusion algorithm, the SINT used to search the critical point was extended to 3.0 seconds. All other parameters for the traditional diffusion algorithm were unchanged.

For the new diffusion algorithm, the searching interval (SINT) Δt was used to search the local maximum lines. The local maximum point was searched within Δt, and the local maximum points are located on the boundary of the critical time interval. Therefore Δt is critical to determine accuracy of the critical time interval. The two different searching intervals Δt 0.33 and 0.21 second were applied to determine whether there is significant change of the critical time interval after SINT has been changed.

3.7.3 Critical Time Interval Reliability Analysis Plan

In order to assess the reliability of the critical time interval, the intraclass correlation coefficient (ICC) index was determined. By comparing the ICC of the traditional and new diffusion algorithms, their reliability can be compared. A higher ICC indicates more consistency and agreement of the associated algorithm, hence it is more reliable. COP data from young adults, both baseline (eyes-close, firm surface) and pre-fatigue trials were used to calculate the ICCs.

3.8 Preliminary Results of the Critical Time Interval for One Participant

COP data, power spectrum and the local maximum power spectrum of wavelet transform for one participant were calculated and shown in Figure 10. Here, the mean value of local maximum intervals is 1.88 seconds. According to previous research (Collins and DeLuca, 1994), empirically the critical time interval should occur within 2.5 seconds. For the mediolateral direction, the critical time interval was 0.63-1.85 seconds, and for the anteroposterior direction the critical time interval was 0.35-1.85 seconds. It was concluded that 1.88 seconds for the critical time interval remains reasonable.

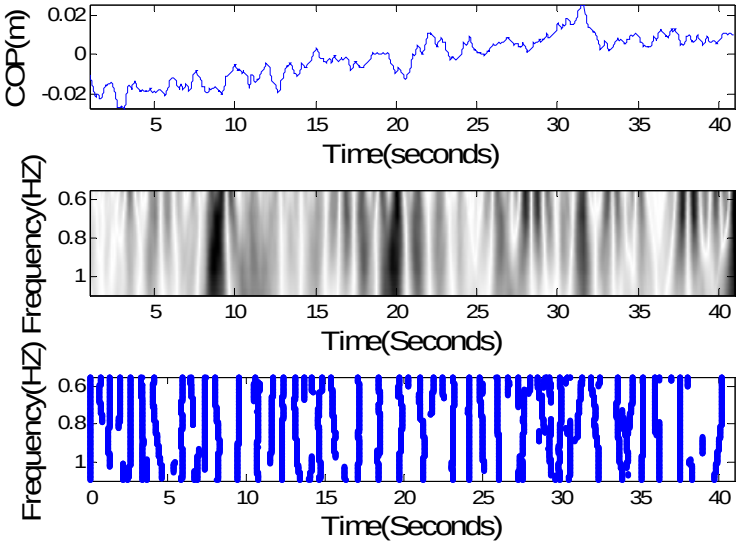

Figure 10: COP data, power spectrum, and the local maximum power spectrum of wavelet transform (Baseline participant 4, eye-open, firm surface, trial 3, ML direction) In Figure 10, the mean value of local maximum intervals is 1.88 seconds.

3.9 Preliminary Comparison of Younger and Older Adults

Results for a young and older adult are shown in Figure 11 and Figure 12. It is apparent that the critical time interval is different between younger (1.50 seconds) and older (0.8 second) individuals. This is taken to imply that the older individual actively (closed-loop)

controlled their upright stance more frequently than young adults. It is also apparent that the magnitude of the older adult COP data is larger than that of the young adult. This may imply that although the older adult more frequently control their posture, their muscle and central nervous systems were not able to respond appropriately to reduce sway magnitude. As a result, the older adult was forced to more frequently to control their sway, resulting in the smaller critical time interval.

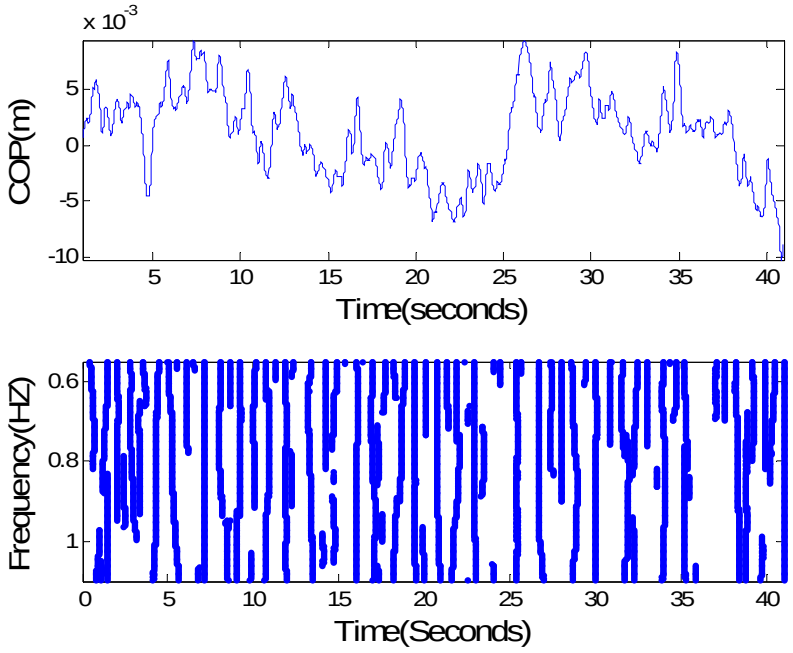

Figure11: COP data, the local maximum power spectrum of wavelet transform (for young adult 11, knee, trial 2, ML direction), the critical time interval is 1.50 seconds.

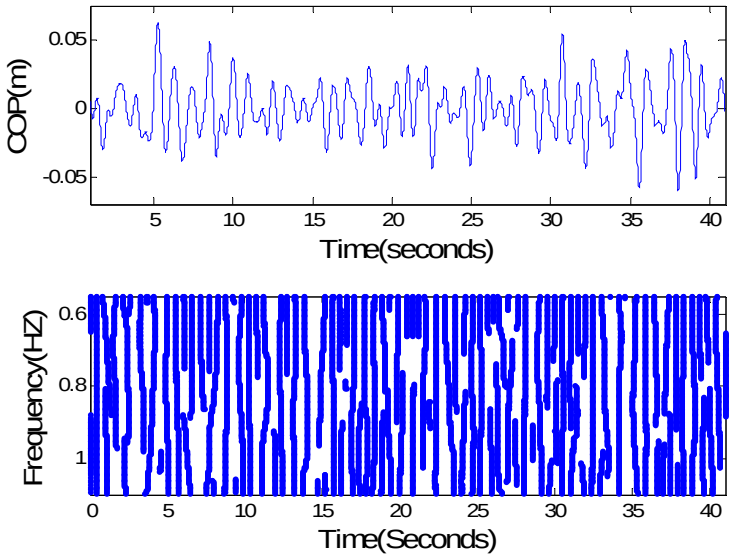

Figure 12: COP data, the local maximum power spectrum of wavelet transform (for older adult 11, knee, trial 2, ML direction), the critical time interval is 0.8 second.

These initial results suggest the feasibility of the new analysis method, and provide some initial indications of age-related differences in postural control. To our knowledge, it is the first time that the upright stance posture control mechanism of young and older adults was identified with a seemingly clear-cut threshold.

Chapter 4 Results

4.1 Effects of Fatigue

Among younger adults, the new diffusion algorithm yielded ML short-term and ML long-term diffusion coefficients that were significantly increased following torso LMF (Figure 13). This implies that torso LMF significantly compromised sway stability. Following ankle, knee and shoulder localized muscle fatigue, both male and female sway intensity was increased. However, LMF induced at these joints do not significantly compromise sway stability. Using the new diffusion algorithm, the range of means of the critical time interval before and after LMF was [1.43, 1.62] seconds and the standard deviation was [0.14, 0.29] seconds.

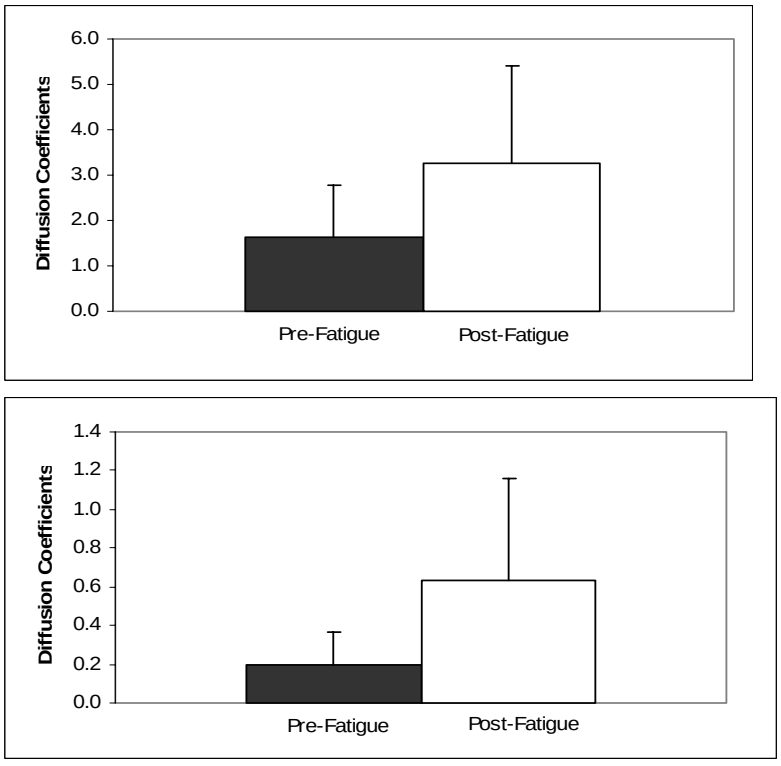

Figure 13: Torso ML short-term and long-term diffusion coefficients (0.01mm^2)

In contrast to the new algorithm, the traditional diffusion algorithm showed that only the ML short-term diffusion coefficients was significantly increased following torso LMF. The traditional diffusion algorithm was not able to detect a significant increase of ML long-term diffusion coefficients after torso LMF. The traditional diffusion algorithm yielded mean values of the critical time interval of [1.22, 1.49] seconds, and a range for the standard deviation of the critical time interval of [0.23, 0.39] seconds.

Among older adults, the new diffusion algorithm showed that, after ankle, knee, torso and shoulder LMF, the ML and AP short-term diffusion coefficients were significantly different between males and females. This suggests that LMF has mediated male and female upright stance control in a different way. Both traditional and new diffusion algorithms showed that diffusion coefficients were not significantly increased after LMF at any joint, therefore it was concluded that most likely localized muscle fatigue has not altered ML and AP upright stance sway stability among the older individuals. The new diffusion algorithm yielded a range for mean of the critical time interval of [0.72, 0.79] second and a range for the standard deviation of the critical time interval of [0.06, 0.13] seconds.

Similarly, LMF at any of the joints did not yield significant differences in diffusion coefficients determined using. This again indicates that ankle, knee, torso and shoulder LMF did not compromise the sway stability of older adults. The traditional diffusion algorithm showed that the range for mean of the critical time interval was [1.04, 1.33]

seconds and the range for standard deviation of the critical time interval was [0.18, 0.38] seconds.

4.2 Effects of Vision and Support Compliance

Baseline conditions consisted of eyes-opened on firm surface (EOF), eyes-closed on firm surface (ECF), eyes-opened on compliant surface (EOC), eyes-closed on compliant surface (ECC). Among the younger participants, the new diffusion algorithm showed that ML and AP short- term diffusion coefficients were significantly smaller under the firm and compliant surfaces with eyes-opened than that under eyes-closed conditions (Figure 14). The AP long term diffusion coefficients were significantly smaller under the compliant surface with eyes opened than the compliant surface with eyes closed (Figure 15). The traditional diffusion algorithm had the same result, where sway intensity on firm and compliant surfaces with eyes-closed condition was larger than that on the firm and compliant surfaces with the eyes-opened condition. These results imply that vision plays an essential role in determining sway stability on both firm and compliant surfaces. In summary, the short-term and long-term diffusion coefficients were not significantly different on firm and compliant surfaces with the same vision conditions. This indicates that sway stability is not significantly different on the different supporting surface conditions when the remaining sensory conditions (vision and vestibular) are the same.

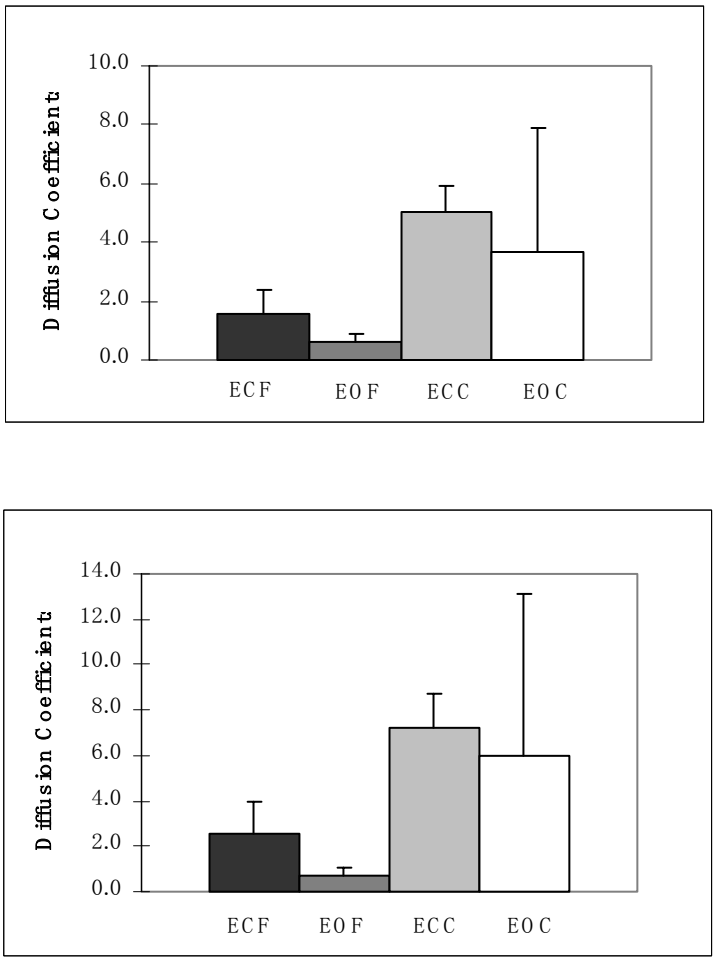

Figure 14: (1) ML short-term diffusion coefficients from the new diffusion algorithm (2) AP short-term diffusion coefficients from the new diffusion algorithm (0.01mm^2)

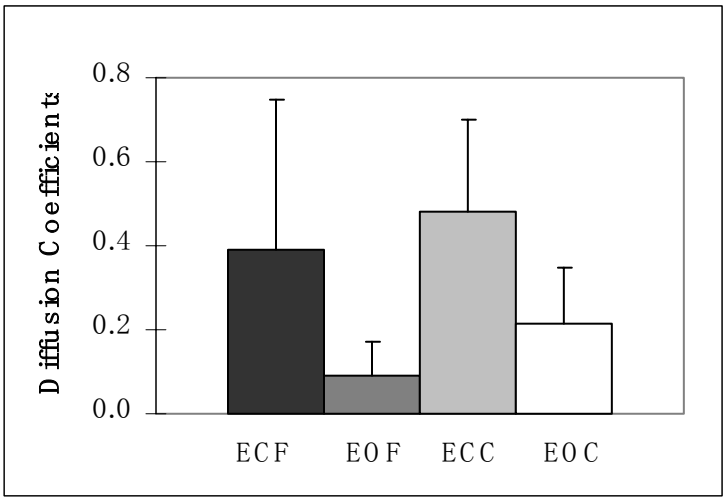

Figure 15: AP long-term diffusion coefficients standing on firm and compliant surfaces with eyes-opened and eyes-closed conditions from the new diffusion algorithm ($0.01 mm^2$)

Among the younger participants, the new diffusion algorithm showed that means of ML critical time intervals were in the range of [0.81-0.92] second, and standard deviations in the range of [0.07-0.13] seconds. From the traditional diffusion algorithm, means of ML/AP critical time interval were in the range of [1.06-1.27] seconds, and standard deviation in the range of [0.36-0.53] seconds. It was apparent that the critical time interval and standard deviations from the new diffusion algorithms was smaller than that from the traditional diffusion algorithm (Figure 16). The critical time interval was not significantly different between the trials on a firm vs. compliant surface. The critical time interval was also not significantly different between with eye-opened vs. eye-closed condition. This indicates that the critical time interval was not tightly dependent on supporting surfaces and visual conditions.

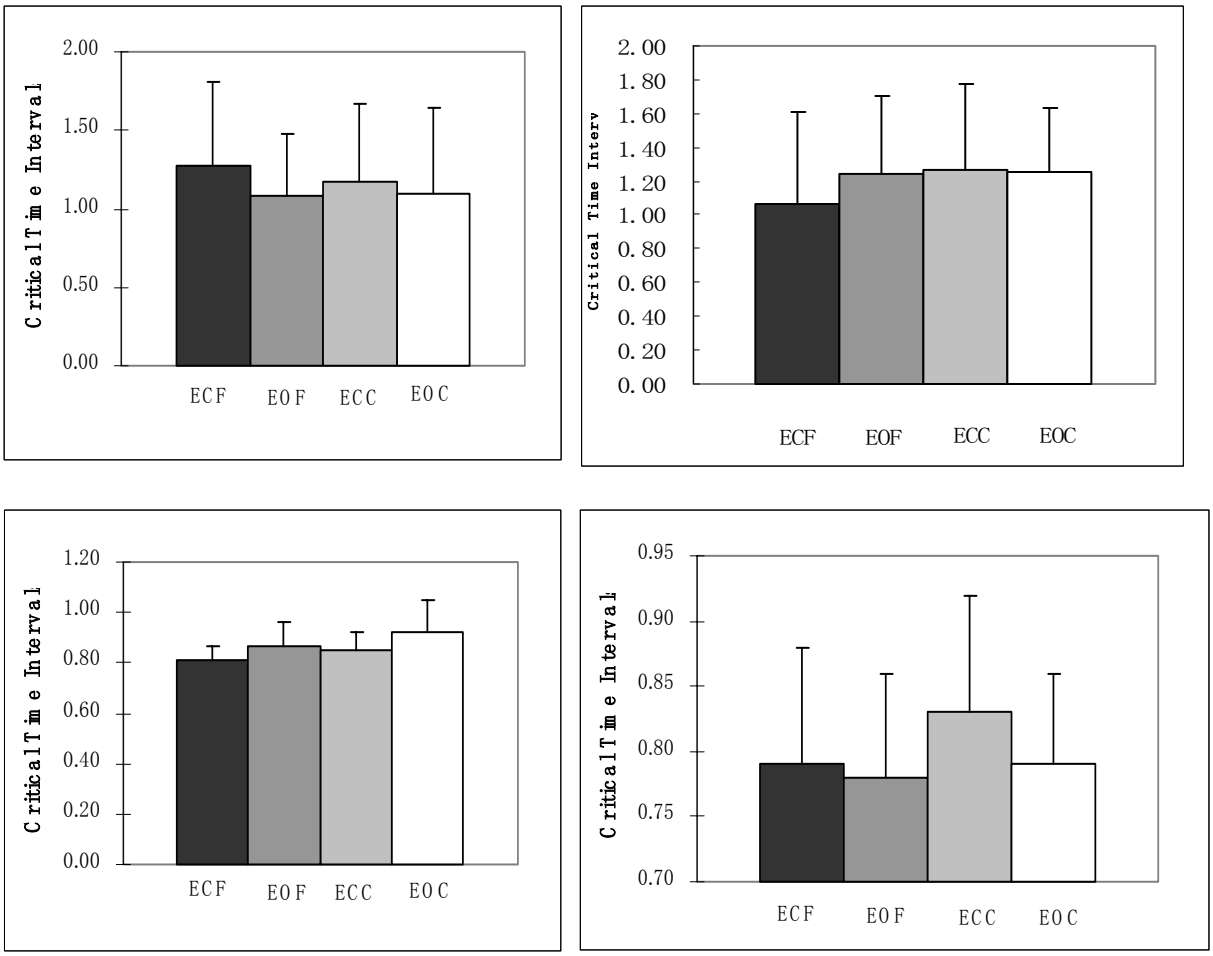

Figure 16: Critical time intervals from the traditional (top graphs) and new (bottom graphs) diffusion algorithms (ML: left; AP; right)

Among the older participants, both the new and traditional diffusion algorithms presented the similar results that the ML and AP short-term diffusion coefficients and the AP long-term diffusion coefficients are significantly different between the upright stance on the firm surface with eye-opened and eye-closed conditions. The same results were also obtained for upright stance on the compliant surface with eye-opened and eye-closed conditions. The older adult diffusion coefficients from the new and traditional diffusion algorithms were presented in Figure 17 and Figure 18.

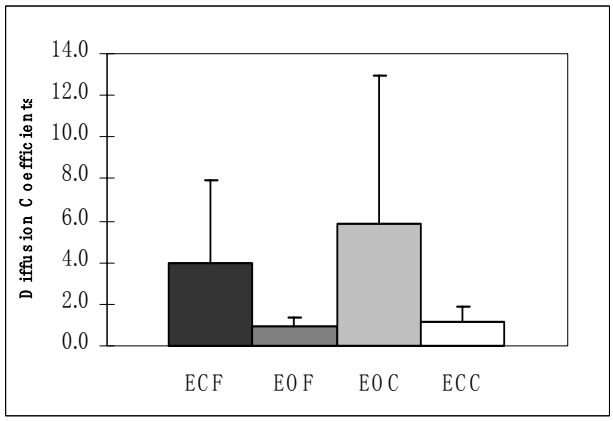

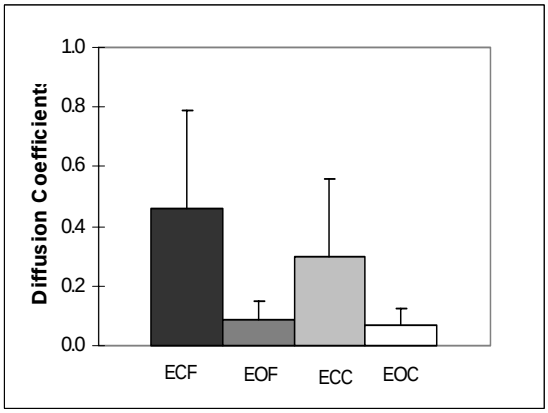

3

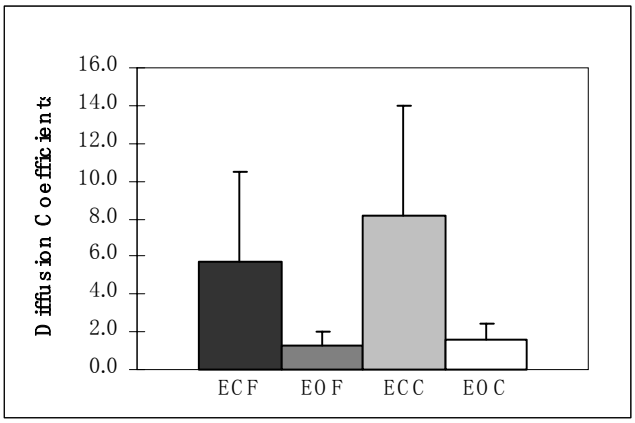

Figure 17: (1) ML short-term diffusion coefficients from the new diffusion algorithm (2) AP short-term diffusion coefficients from the new diffusion algorithm (3) AP long-term diffusion coefficients from the new diffusion algorithm **(** 0.01mm^2 **)**

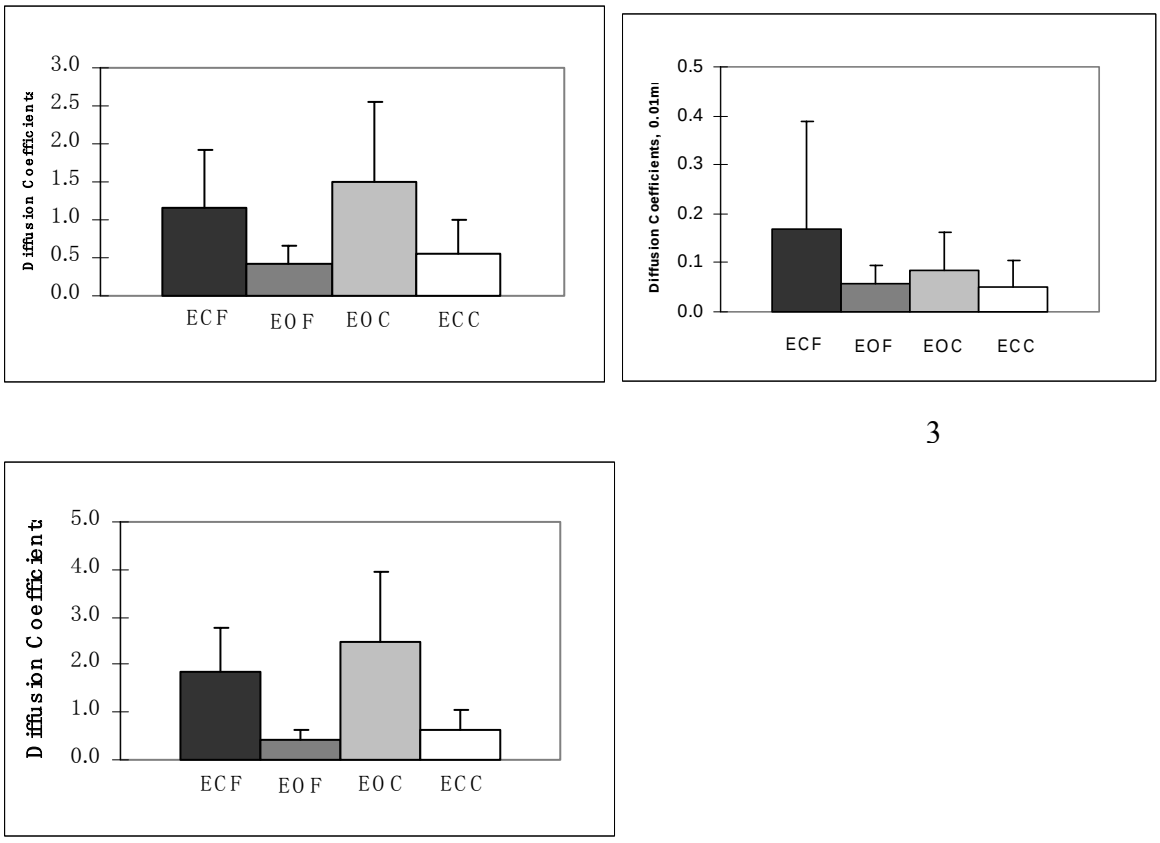

3

Figure 18: (1) ML short-term diffusion coefficients from the traditional diffusion algorithm (2) AP short-term diffusion coefficients from the traditional diffusion algorithm (3) AP long-term diffusion coefficients from the traditional diffusion algorithm (0.01mm^2)

Among the older participants, critical time intervals from the new diffusion algorithm and the traditional diffusion algorithm were presented in Figure 19. The traditional diffusion algorithm showed that mean of ML/AP critical time interval is in the range of [1.1-1.38] seconds, standard deviation is in the range of [0.31-0.59] second. The new diffusion algorithm showed that mean of ML critical time intervals is in the range of [0.71-0.85]

second, and standard deviation is in the range of [0.06-0.14] second. It is apparent that the standard deviation from the new diffusion algorithm is much smaller than that from the traditional diffusion algorithm.

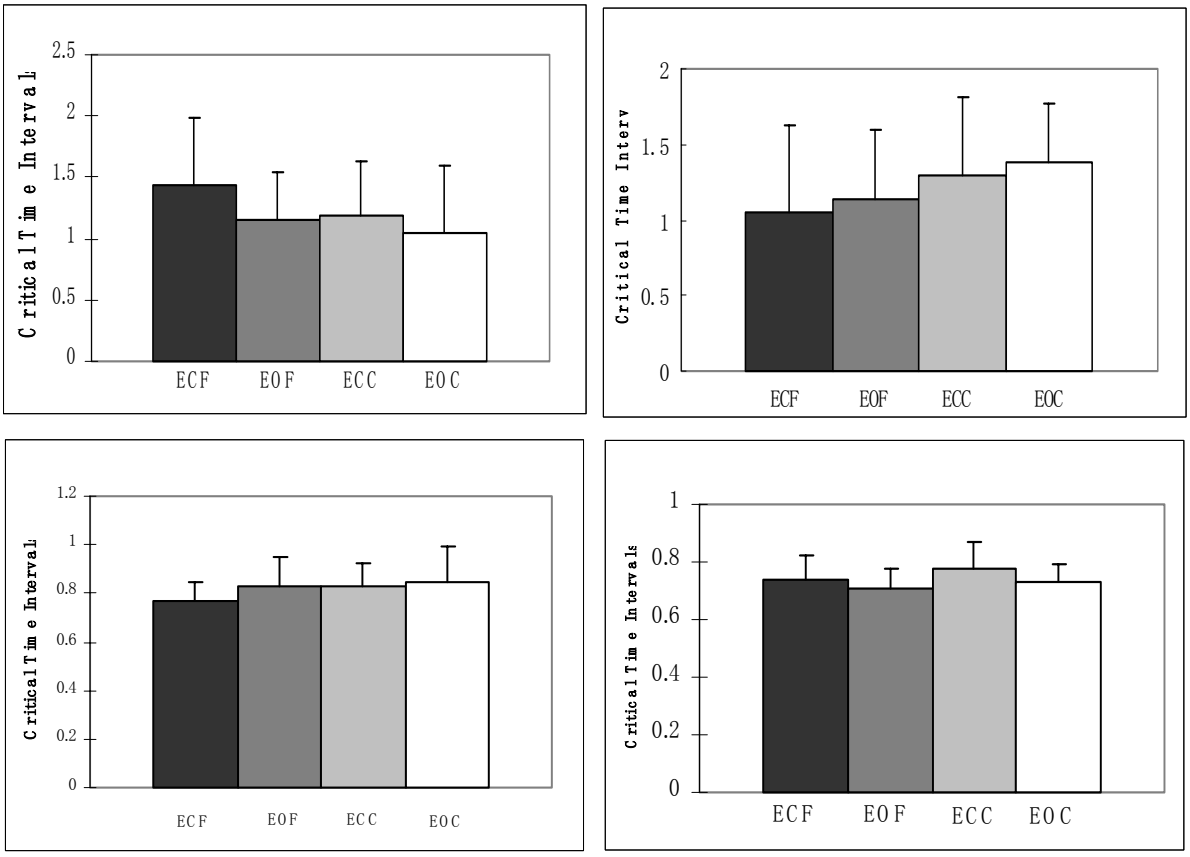

Figure 19: Critical time intervals from the traditional (top graphs) and new (bottom graphs) diffusion algorithms (ML: left; AP; right)

4.3 Critical Time Interval Sensitivity Analysis

Data from the younger adults, including ankle, knee, torso and shoulder LMF, were used in critical time interval sensitivity analysis. In the traditional critical time interval identification method, the searching intervals (SINT) used to search for the critical time interval were 2.5 seconds and 3 seconds. The mean value of pre-fatigue (1-3 trials) and

the mean value of post-fatigue (5-7 trials) critical time interval with respect to ML and AP directions were calculated. Results showed that the change of the critical time interval is in the range $[\pm 0.05, \pm 0.26]$ seconds. In the new critical time interval identification method, the searching intervals (SINT) used to search for critical time interval were 0.21 second and 0.33 second. The mean value of pre-fatigue (1-3 trials) and the mean value of post-fatigue (5-7 trials) critical time interval with respect to ML and AP directions was calculated. The results showed that the change of the critical time interval is in the range of $[\pm 0.01, \pm 0.03]$ second.

It is thus apparent that after the searching interval (SINT) was changed, changes in the critical time intervals obtained from the new identification algorithm were much smaller than that from the traditional dentification algorithm. This result indicates that the new diffusion algorithm is not as sensitive as the traditional diffusion algorithm to changes of SINT.

4.4 Reliability Analysis

Both baseline and pre-fatigue trials were used in the critical time interval reliability (ICC) calculations. The results (Tables 2 and 3) indicated reliability of the critical time interval using the new diffusion algorithm was generally better (larger ICC index) across visual and surface conditions than that from the traditional diffusion algorithm for both young and older adults. These difference, however, were dependent on the sensory conditions. The new diffusion algorithm showed more reliable critical time intervals than the traditional diffusion algorithm for experimental session data (Table 4). Across the range

of data, the new diffusion algorithm yielded more consistent ICCs [0.225-0.48] compared with the traditional diffusion algorithm [0.121-0.585].

Table 2: ICC values for young adults during the baseline study

	ECF	EOF	ECC	EOC
New Diffusion Algorithm	0.133	0.406	0.885	0.276
Traditional Diffusion Algorithm	0.136	-0.738	0.283	0.272

Table 3: ICC values for older adults during the baseline study

	ECF	EOF	ECC	EOC
New Diffusion Algorithm	0.674	0.459	0.614	0.403
Traditional Diffusion Algorithm	0.484	0.161	-0.294	0.317

Table 4: ICC values for young adults during the experimental session (pre-fatigue)

	ECF (Day1)	ECF(Day2)	ECF(Day 3)	ECF(Day 4)
New Diffusion Algorithm	0.48	0.356	0.225	0.428
Traditional Diffusion Algorithm	0.264	0.585	0.121	0.214

4.5 Short-term Hurst Exponent

Among younger adults, and after ankle, knee, torso and shoulder LMF, no significant changes in short-term exponents were observed. Most of the post-fatigue Hurst exponents, however, were smaller than pre-fatigue values. This result is not in agreement with the result from both traditional and new diffusion algorithms, where significant increases in diffusion coefficients were identified following torso LMF. Therefore, it was

concluded that the short-term Hurst exponent may not be valid to detect LMF effects on upright stance stability.

Chapter 5 Discussion

Our research aimed at understanding the effects of localized muscle fatigue on sway stability. In order to realize this objective, a new diffusion algorithm was proposed to address drawbacks of the traditional diffusion algorithm. An increased diffusion coefficient was regarded as an indicator of decreased sway stability. Results as a whole showed that that torso LMF significantly affected sway stability. The torso muscles play an important role in maintaining the sway stability. Kuukkanen and Maikia (2000) indicated that low back pain patients exhibited an increased sway velocity after home exercises. Simo et al., (1999) conducted an experiment in which participants performed repetitive trunk extensions against resistance until exhaustion. It was concluded by them that lumbar fatigue impairs the human ability to sense position change. More specifically, Davidson et al., (2004) showed an increase up to 58% in time-domain posture sway measures (e.g., mean velocity, sway area) following lumbar extension fatigue. Consistent with these results, our present results showed that torso LMF has impaired postural stability. In addition, it has been suggested that the hip is more responsible for controlling ML sway (e.g., Winter, 1995; Henry et al., 1998). Similarly, our results showed that both ML short-term and long-term diffusion coefficients increased significantly due to impairments from torso LMF.

Whipple et al., (1987) indicated that weakness of the knee and ankle is correlated with falls. However, in our study, there was no significant impairment of sway stability observed after the ankle and knee LMF. This perhaps was due to the fact that the ankle

and knee exercises (used to induce LFM) were not sufficient to significantly compromise stability. During ankle fatigue exercises, the soleus muscle was fatigued. The fatigued soleus muscle leads to a compromised sway posture in AP direction (Mochizuki et al., 2005). Our results also showed (though not significantly) that following ankle localized muscle fatigue there was a greater increase in AP vs. ML sway. In summary, our research showed that torso plays much more important role in sway posture control than ankle and knee.

Christon and Garlton (2001) compared young and elderly individual motor variability after continuous and rapid discrete isometric contractions. It was found that during continuous isometric contractions, young and elderly individuals exhibited similar isometric contraction coefficients of variation (CV). In contrast, during rapid discrete isometric contractions, the elderly individuals exhibited higher CVs than young individuals. This implies that the elderly have similar muscle performance during continuous isometric contractions. Tracy and Enoka (2002) showed that coefficient of variation of old adults is greater than that of young adults at 2, 5, and 10% of MVC. However, the fluctuation of knee joint angle during slow motions was similar to young adults. The continuous isometric and slow motions did not reduce the older adult's physical performance. These two study results revealed that, after exercises, older adults show lower muscle and physical performance only with respect to specific features (e.g., abrupt motion).

Skinner et al., (1986) indicated that the muscle receptors were particularly compromised by LMF. In contrast, they pointed out that LMF possibly causes an increased sensitivity of capsular receptors. This implies that, following LMF, stability was not necessarily deteriorated due to an impairment of muscle receptors, considering the increased sensitivity of capsular receptors. In addition, Woollacott et al., (1986) studied participants of varying age (20~70 years old), and reported that the contributions from sensory inputs to balance were not progressively altered with aging. This evidence possibly explains why there was no significant increase in postural sway posture after LMF among older adults. Furthermore, Horak & Nashner (1986) indicated that people are able to coordinate the ankle and hip strategies to adapt to current support-surface conditions and recent experiences. This result indicates that upright sway is controlled by central programming. In our study, the exercise level might not have caused fatigue in older adult central programming, which turns out to adequately control sway.

Krishnamoorthy and Yang (2005) indicated that joint configuration variance was significantly lower under eyes-opened (EO) than eyes-closed (EC) conditions. The authors provided joint strategies to explain why there was less sway stability observed in EC vs. EO conditions. Blaszczyk et al., (1993) reported that elderly individuals showed significantly greater ML center of gravity oscillation than young individuals. Similarly, Fitzpartrick and McCloskey (1994) indicated that vision provides critical sensitive sway perception for certain velocities of upright standing. These are consistent with our finding that in the baseline test, the older adults sway showed greater short-term diffusion coefficients in both ML and AP directions than young adults. Furthermore, our study

also found that both young and older adult diffusion coefficients were much larger under the EC than EO conditions.

The objective for testing sway on both firm and compliant surfaces was to determine whether the different proprioceptive feedback will result in different sway control. Fitzpartrick and McCloskey (1994) concluded that proprioception from legs provided the most sensitive perception for normal upright standing sway. Hence, different proprioception conditions may cause different sway. From our results, there was an increase in sway (not significant) observed on the compliant surface compared with the firm surface. This demonstrates that compromised proprioception may have mediated sway. The likely underlying causes for this are given in the following. Fujisawa et al., (2005) indicated that the central nervous system selectively chooses from the ankle and hip somatosensory feedback paths to control postural sway. The compliant surface condition in our baseline can only deteriorate the ankle somatosensory feedback path to a certain level, but a normal hip somatosensory feedback path was retained. The central nervous system could still include the hip somatosensory feedback pathway to compensate for the ankle proprioception loss. In addition, our results are consistent with research from Pyykko et al., (1990). The complaint surface situations in their studies did not significantly compromise sway stability.

The critical time interval calculated with the new diffusion algorithm was different from that from the traditional diffusion algorithm. The critical time interval from the traditional diffusion algorithm is roughly similar between young and older adults.

However, from the new diffusion algorithm, the young adults' critical time interval mean value was 1.43~1.62 seconds, and the standard deviation was 0.12~0.29 seconds. The older adults' critical time interval mean value was 0.72~0.82 second, and the standard deviation was 0.06~0.13 seconds. It is apparent that the young adults have much larger critical time interval mean value as well as standard deviation than the older adults. This is a new finding from our research. There is as yet no systematic mechanism formed by other research studies to explain this phenomenon. In our study, the critical time interval is the period of proprioceptive postural control. The smaller critical time interval values from older adults reflects that older adults more frequently activated the proprioceptive portion of their posture control systems. The more frequent proprioceptive activation may arise from three sources. Firstly, proprioception was deteriorated following the LMF. Compensation for such deterioration forces proprioception to be activated more frequently. Secondly, central fatigue may also contribute to the abrupt increase of the frequency for proprioception control. Thirdly, weakness of muscles may also be responsible for the increase in frequency of proprioception control. More details have to be investigated to confirm the underlying physiology used to determine the frequency of proprioception.

During the baseline study, young and older adults critical time intervals (standard deviation) were respectively 1.00-1.43 (0.39-0.58) and 0.71-0.92 (0.06-0.45) seconds. It is apparent that the older adult critical time interval and standard deviation were smaller than the young adults. The same interpretation above can be given for this phenomenon.

The traditional diffusion algorithm was not able to distinguish the young and older adult critical time interval with a clear-cut threshold. Through the new diffusion algorithm, a clear-cut threshold of critical time intervals between the young and older adult was identified. It is still not possible to give specific reasons for such results, due to the limited available literature discussing it.

The new critical time interval identification algorithm was not as sensitive as the traditional critical time interval identification algorithm to changes in the searching interval (SINT). The reason is that the new diffusion algorithm searched a small interval (about 2.5 seconds) to get the local maximum. Statistically, the relatively small sample size from this interval often results in large variation. In contrast, the new critical time interval identification algorithm searches throughout the entire data sample instead of a partial data sample as the traditional algorithm does. Therefore, the variation is smaller than that of the traditional algorithm.

The new algorithm yielded more consistent critical time intervals than the traditional algorithm. This is because the two algorithms are based on different assumptions about the physiology of sway control. The searching technique in the traditional algorithm is not able to reflect upright stance control mechanisms, since muscle and tendon stiffness effects on sway posture were not eliminated from the data. On the contrary, the new algorithm was designed based on the physiological context, and the stiffness effects on sway were eliminated. Other sway control mechanisms except proprioception (e.g., the vision and central nervous systems) were also eliminated. Therefore, the critical time

interval identified from new diffusion algorithm only reflected the period of proprioceptive control of sway.

It was found that the short-term Hurst exponent was not valid to detect LMF effects. This is likely because the short-term Hurst exponent used only a small sample of COP data, leading to a large variation of Hurst exponents compared with existing results using more extensive COP data. This result is consistent with the comment from Michel and Matt (2005), who argued that with a larger sample size, more accuracy will be achieved by the Hurst exponent algorithm.

Chapter 6 Conclusions and Future work

In this research, a new algorithm for determining the critical time has been developed for the diffusion algorithm. The objective for developing this algorithm was to more precisely identify the diffusion coefficients that characterize the control of postural sway. A good understanding of this control can serve, in the long term, to better prevent risks of occupational falls.

Diffusion data, which are the auto-correlation of the COP data, are in the time domain. The time domain signal is the summation of sub-signals across frequency bands. Studies have revealed that the diverse inputs to sway control mechanisms (e.g., vision, proprioception, vestibular, and central nervous system) are related to different frequency bands. It was therefore derived that the sway control mechanisms can be identified through analyzing the properties of these frequency bands. As shown in Figure 20, vision, vestibular and proprioception feedback controllers have been assumed, where the central nervous system is a plant.

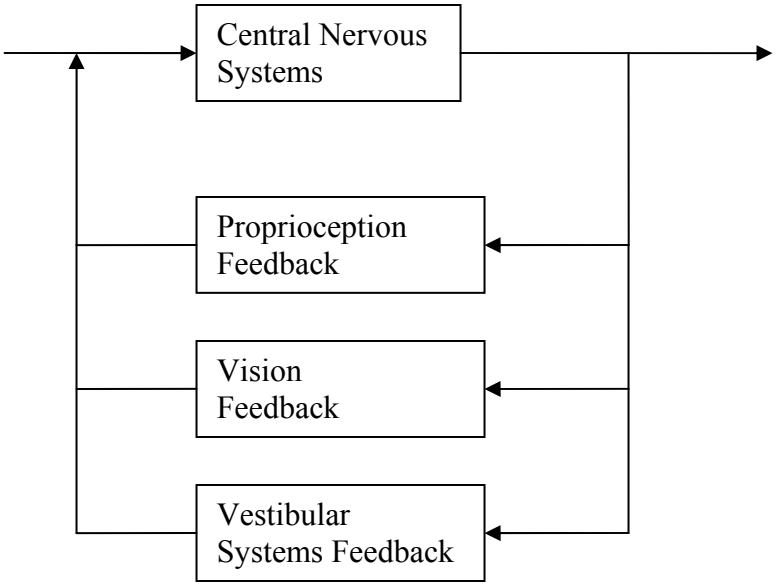

Figure 20: Postural control Feedback Mechanism

It has been widely accepted that propioception is compromised by LMF. By analyzing the frequency band related to proprioception in pre-fatigue and post-fatigue COP data, the effects of LMF on proprioception can be identified. The local maximum line is a set of local maxima in COP data, across the frequency bands (0.5-1.0 HZ) at a specified time. The local maximum in COP data is a transit point, which indicates that there is an oppositely directed motion before and after this point. As shown in our preliminary results, the local maximum lines have a similar interval. This implied that proprioception feedback control was used periodically. The critical time interval was defined as the period where no significant feedback control was identified. Primary feedback control occurred closely around the local maximum lines, therefore the interval between the local maximum lines was the critical time interval.

The critical time interval was used to distinguish between short-term and long-term diffusion. Both short-term and long-term diffusion coefficients are crucial to describe

sway control (being associated with open- and closed-loop control, respectively). In other words, they are respectively used for describing sway control without and with feedback. An improved estimation of the critical time interval is essential to enhance the precision of diffusion coefficients, and subsequently any interpretation regarding the control process.

After applying the new critical time interval method to the diffusion algorithm, our results showed that the mean and standard deviation of critical time intervals for older adults are significantly smaller than for young adults. This phenomenon may have resulted from the weakness of muscles, the reduced performance of central control or proprioception. However, there is as yet no strict interpretation for this age-related effect. This phenomenon may, however, explain why older adults fall more frequently than younger adults. There were no statistically significant changes in critical time intervals following LMF. However, it was found that LMF among young adults usually caused the critical time interval to be decreased. In contrast, the LMF among older adults caused the critical time interval to be increased.

The diffusion coefficients showed that LMF among young adults increased following torso LMF. There were no significant increases of diffusion coefficients observed for older adults following LMF. This suggests that the older adults were more resistant to the effects of LMF. Although sway of older adults was not impaired following LMF, this does not mean that LMF cannot compromise the sway stability in older adults. More

prolonged duration and increased exercise loads may actually compromise stability in this group as well.

Vision was found to play a crucial role in determining sway stability. Diffusion coefficients with the eyes-closed were significantly larger than those with the eyes-opened. This may help explain why the poorer vision of older adults contributes to falls. There were no significant difference in sway resulting from the different supporting conditions (complaint surface and firm surface). This implies that the supporting surface conditions do not significantly compromise sway stability.

It was found that the short-term Hurst exponent was not valid to detect LMF effects on sway stability. It appears that the Hurst exponent algorithm requires a large sample of COP data to ensure its accuracy. In contrast, the diffusion algorithm needs a relatively smaller sample of COP data.

Possible future work can be conducted in the following two areas. There is a need to identify the causes of the smaller critical time intervals among older adults. This might have resulted from different central control, muscle weakness, or different proprioception mechanisms, but the present study was not able to differentiate among these underlying causes. There is also a need to explore underlying mechanism for why older adults were more resistant to LMF. It might be that older adults have more reliable central control systems that are able to better coordinate hip and ankle sway strategies.

References

[1] American Geriatrics Society, British Geriatrics Society, and American Academy of Orthopaedic Surgeons Panel on Falls Prevention. Guidelines for the Prevention of Falls in Older Persons. New York, 2001.

[2] Bagchee, A., & Bhattacharya, A. (1998). Postural stability assessment during task performance, Occupational Ergonomics. 1(1):51-53

[3] Blaszczyk, J.W., Hansen, P.D., Lowe, D.L., (1993). Postural sway and perception of the upright stance stability borders. 22(11): 1333-1341

[4] Brill, J.C., Hancock, P.A., & Gilson, R.D., (2003). Driver fatigue: is something missing?, Proceedings of the Second International Driving Symposium on Human Factors in Driver Assessment, Training and Vehicle Design.

[5] Carroll, J. and Freedman, W., (1993). Nonstationary properties of postural sway, J. Biomech. 26(415): 409-416

[6] Caron,O., (2004) Is there interaction between vision and local fatigue of the lower limbs on postural control and postural stability in human posture?, Neurosci Lett. 363(1):18-21

[7] Christou, E.A.,& Carlton, L.G., (2001). Old adults exhibit greater motor output variability than young adults only during rapid discrete isometric contractions, Journal of Gerontology: Biological Sciences, 56A(12): B524-B532

[8] Clark, M., Jackson, P.,&cohen, H.H., (1996). What you don't see can hurt you: understanding the role of depth perception in slip, trip, and fall incidents, Ergonomics in Design. 4(3):16 -21.

[9] Collins, J.J.,& De Luca, C.J., (1993). Open-loop and closed-loop control of posture a random-walk analysis of center-of-pressure trajectories, Experimental Brain Research. 95(2):308–318

[10] Collins, J.J.& DeLuca, C.J., (1994). Random walking during quiet standing, Physical Review Letters. 73(5):764-767

[11] Collins, J.J.,& De Luca, C.J., (1995a). The effects of visual input on open-loop and closed-loop postural control mechanisms, Experimental Brain Research. 103(1):151-63

[12] Collins, J.J.,&De Luca, C.J., (1995b). Upright correlated random walks a statistical-biomechanics approach to the human postural control system, Chaos. 5(1):57–63

[13] Collins, J.J., De Luca, C.J., Burrows, A., & Lipsitz, L.A.,(1995). Age-related changes in open-loop and closed-loop postural control mechanisms, Experimental Brain Research. 104(3):480-92

[14] Coyle, E. F., Coggan, A.R., Hemmert, M.K., & Ivy, J. L., (1986). Muscle glycogen utilization during prolonged strenuous exercise when fed carbohydrate, J Appl Physiol. 61(1):165-172

[15] Daniel, O.C., Benjamin, M.,& Tabak, B., (2004). The Hurst exponent over time: testing the assertion that emerging markets are becoming more efficient, Physica A: Statistical and Theoretical Physics. 336(3-4):521-537

[16] Davidson, B.S., Madigan, M.L., &Nussbaum, M.A., (2004). Effects of lumbar extensor fatigue rate on posture sway, J Appl Physiol. 93(1-2):183-189

[17] Deschenes,M.R.,(2004).Effects of aging on muscle fibre type and size, Sports Medicine. 34(12):809-824

[18] Dietz, V., (1992). Human neuronal control of automatic functional movements: Interactions between central programs and afferent input, Physiological Reviews. 72(1):33–69

[19] Dietz,V., Maurtz, K.H.,&Dichgans, J., (1980). Body oscillations in balancing due to segmental stretch reflex activity, Exp Brain Res. 40(1):89-95

[20] Diener, H.C., Dichgans, J.,Bootz, F., &Bacher, M., (1984). Early stabilization of human posture after a sudden disturbance: influence of rate and amplitude of displacement, Exp Brain Res. 56(1):126-134

[21] Doyle T.L., Newton M.R., Burnett A.F., (2005). Reliability of traditional and fractal dimension measures of quiet stance center of pressure in young healthy people, Arch Phys Med Rehabil. 86(10):2034:2040

[22] Duarte, M.,& Zatsiorsky, V.M., (2000). On the fractal properties of natural human standing, Neuroscience Letters. 283(3):173-176

[23] Ferdjallah, M.,Gerald, F.,Jacqueline,H.,& Wertsch, J., (1999). Instantaneous postural stability characterization using time-frequency analysis, Gait & Posture.10(2):129-134

[24] Fitzpatrick, R., & McCloskey, DI., (1994). Proprioceptive,visual, and vestibular threshold for the perception of sway during standing in humans, Journal of physiology. 478(1):173-186

[25] Fujisawa,N., Masuda,T.,Inaoka,Y.,Fukuoka,H.,Ishida,A.,Minamitani,H., (2005). Human standing posture control system depending on adopted strategies, Med Biol Eng Comput. 43(1):107-114

[26] Gagery, P.M., Bizzo,G., Debruellle,O., &Lacroix, D., (1985). The one hertz phenomenon in vestibular control on posture and locomotor equilibrium. Igarashi,M., & Black, F.O., Eds, (Karger, basel). 89-92

[27] Hargreaves, M., (1992). Metabolic factors in fatigue, Sports Med. 13(2):99-107

[28] Hasan, S.S., Robin, D.W., Szurkus, D.C., Ashmead, D.H., Peterson, S.W., & Shiavi, D.R.G., (1996). Simultaneous measurement of body center of pressure and center of gravity during upright stance, Part II: Amplitude and frequency data. 4(1): 1-78

[29] Hausdorff, J.M., Rios,D.A., &Edelber, H.K., (2001). Gait variability and fall risk in community-living older adults: a 1-year prospective study, Archives of Physical Medicine and Rehabilitation. 82(8):1050–1056

[30] Henry,S.M., Fung,J.,&Horak,F.B., (1998) Control of stance during lateral and anterior/posterior surface translations, IEEE Trans Rehab Engr. 6(1):32–42.

[31] Hertel, J., & Olmsted-Kramer, L.C., (2006). Deficits in time-to-boundary measures of postural control with chronic ankle instability, Gait & Posture, Article in Press

[32] Horak, F.B., and Nashner, L.M., (1986). Central programming of postural movements: adaptation to altered support surface configurations, Journal of Neurophysiology. 55(6):1369-1381

[33] Hornbrook, M.C., Stevens, V.J., Wingfield, D.J., Hollis, J.F., Greenlick, M.R., &Ory, M.G., (1994). Preventing falls among community-dwelling older persons: results from a randomized trial, The Gerontologist. 34(1):16–23

[34] Jaffard, S., (1997). Multifractal formalism for functions part i: results valid for all functions, Siam J. Math. Anal. 28(4): 944-970

[35] Johansson, R., memberie, E.E., Magnusson, M. A., and Akesson, M., (1988). Identification of human postural dynamics, IEEE transactions on biomedical engineering. 35(10):858-869

[36] Johansson, R., & Magnusson, M., (1991). Human postural dynamics, Crit Rev Biomed Eng. 18(6): 413-437

[37] Joseph, B.M., Kevin, M. G., Robert,A.S., &William,E.P.,(1999). Proprioception and Neuromuscular Control of the Shoulder After Muscle Fatigue, J Athl Train.34(4): 362–367.

[38] Kent-braun, Ng, A.V., Doyle, J.W., &Towse, T.F., (2002). Human skeletal muscle responses vary with age and gender during fatigue due to incremental isometric exercise, J Appl Physiol. 93(5):1813–1823

[39] Krishnamoorthy, V., Yang, J.F., (2005). Joint coordination during quiet stance: effects of vision, Exp brain Res, 164(1):1-17

[40] Kuo, A.D., (1995). An optimal control model for analyzing human postural balance, IEEE transactions on biomedical engineering. 42(1):87-101

[41] Kuukkanen, T.M., & Maikia, E.A., (2000). An experiment controlled study on postural sway and therapeutic exercise in subjects with low back pain, Clin Rehabil. 2000(14): 192-202

[42] Lepers,R., Bigard,A.X.,Diard, J-P.,Gouteyron,J-F., Guezennec,C.Y., (1997). Posture control after prolonged exercise, European Journal of Applied Physiology and Occupational Physiology, 76(1):55-61

[43] Lipsitz , L.A., (2002). Dynamics of Stability: The physiology basis of functional health and frailty, Journal of Gerontology: Biological Sciences. 57A (3): B115-B125

[44] Loughlin, P., Redfern, M., & Furman, J., (1996). Time-varying characteristics of visually-induced postural sway, IEEE Trans. Rehab. Engr. 4(4): 416-424

[45] Maki, B. E. and McIlroy,W. E.,(1996). Postural control in the older adult, Clinical geriatric medicine.12(4): 635-658

[46] Mandelbrot, B.B., &Van Ness, J.W., (1968). Fractional Brownian motions, fractional noises and applications, SIAM Re. 10(4): 422–437

[47] Massion, J., (1994). Postural control system, Curr Opin Neurobiol. 4(6):877-887

[48] Michel, C., & Matt, D.,(2005). A comment on measuring the Hurst exponent of financial time series, Physica A: Statistical and Theoretical Physics. 348(15): 404-418

[49] Minor, L.B., (1998). Physiological principles of vestibular function on earth and in space, Otolaryngology - Head and Neck Surgery. 118(3):S5-S15

[50] Miura, K., Ishibashi, Y., Tsuda, E., Okamura, Y., Otsuka, H., and Toh, S., (2004). The effect of local and general fatigue on knee proprioception, Arthroscopy: The Journal of Arthroscopic & Related Surgery. 20(4): 414-418

[51] Mochizuki,G., Ivanova,D., &Garland, J., (2005). Synchronization of motor units in human soleus muscle during standing postural tasks, J neurophysiology. 94(1): 62-69

[52] Muzzy, J.F., Bacry, E.,& Arneodo, A.,(1993). Multi-fractal formalism for fractal signals: The structure-function approach versus the wavelet-transform modulus-maxima method, Physical Review E. 47(2):875-884

[53] Nicolas, F., Normand, T., & Vincent, N.,(2002).Alteration of the position sense at the ankle induced by muscular fatigue in humans, Medicine & Science in Sports & Exercise. 34(1):117-122

[54] Norrisa, J.A., Marshb, A.P., Smithb, I.J., Kohutc, R.I., & Millerd, M.E., (2005). Ability of static and statistical mechanics posturographic measures to distinguish between age and fall risk, Journal of Biomechanics. 38(6): 1263-1272

[55] Nybo, L., (2003). CNS fatigue and prolonged exercise: effect of glucose supplementation, Med Sci Sports Exerc. 35(4):589-94

[55] Pavol, M.L., Owings, T.M., Foley, K.T., Grabiner, M.D., (2001). Mechanism leading to a fall from an induced trip in healthy older adults, Journal of Gerontology: Medical Sciences. 56A(7):M428-M437

[56] Pfeifer, M., Begerow, B., Minne, H.W., Schlotthauer, T., Pospeschill, M., Scholz, M., Lazarescu, A.D., &Pollahne, W., (2001). Vitamin D status, trunk muscle strength, body sway, falls, and fractures among 237 postmenopausal women with osteoporosis, Exp Clin Endocrinol Diabetes. 109(2):87-92.

[57] Pyykko, I., Jantti, P., and Aalto, H., (1990). Postural Control in Elderly Subjects, Age Ageing. 19: 215-221

[58] Phillip,A.G., & Hertel,J., (2004). Effect of hip and ankle muscle fatigue on unipedal postural control, Journal of Electromyography and Kinesiology. 14(6):641-646

[59] Phillip,A.G.,& Hertel, J., (2004). Effect of lower-extremity muscle fatigue on postural control, Archives of Physical Medicine and Rehabilitation. 85(4):589-592

[60] Pierre-Jean, L., Petrella, R.J., Sproule, J.R., Fowler, P.J., (1997). Effects of Fatigue On Knee proprioception, Clinical Journal of Sport Medicine. 7(1):22-27

[61] Plamen, ch.I.,Nunes Amaral,A.l., Goldberger,S.H.,Rosenblum,M.G.,Struzik,Z.R., &Stanley, H.E., (1999) Multifractality in human heartbeat dynamics, Nature. 399(6735):461-465

[62] Prieto, T.E., Myklebust, J.B., Hoffmann, R.G., Lovett, E.G., & Myklebust, B.M., (1996). Measures of postural steadiness: differences between healthy young and elderly adults, IEEE Transactions on Biomedical Engineering. 43(9): 956-966.

[63] Redfern, S., Furman, M.S., El-Jaroudi, J.M.,&Chaparro,A.,(1995). Time-frequency analysis of postural sway, Journal of Biomechanics. 28(5):603-607

[64] Riddle, D.L., & Stratford, P.W., (1990). Interpreting validity indexes for diagnostic tests: an illustration using the berg balance test. Phys Ther. 79(10): 939-948

[65] Schmuckler, M.A., (1997). Children's posture sway in response to low and high frequency visual information for oscillation, Journal of Experimental Psychology. 23(2):528-544

[66] Simo, T., Markku, K., Satu, L., (1999). The effect of lumbar fatigue on the ability to sense a change in lumbar position: a controlled study, exercise physiology and physical examination, Spine. 24(23):1322-1327.

[67] Sjøgaard, G., Savard, G.,& Juel,C. (1988). Muscle blood flow during isometric activity and its relation to muscle fatigue, European Journal of Applied Physiology (Historical Archive). 57(3):327–335

[68] Skinner, H.B., Wyatt, M.P., Hodgdon, J.A., Conard, D.W., &Barry. R. l., (1986). Effect of fatigue on joint position sense of the knee, Journal of orthopaedic research. 4(1):112-118

[69] Thurner, S., Mittermaier, C., Hanel, R., & Ehrenberger, K., (2000). Scaling-violation phenomena and fractality in the human posture control systems, Phys. Rev. E. 62(3): 4018–4024

[70] Tian, J., & Wells, Jr, R. O., (1995). Vanishing moments and wavelet approximation, Tech. Rep. CML TR95-01, Computat. Math. Lab., Rice Univ., Houston, TX

[71] Tracy, B.L., & Enoka, R.M., (2002). Older adults are less steady during sub-maximal isometric contractions with the knee extensor muscles, J Appl Physiol 92(3):1004-1012

[72] Westerblad, H., Allen, D.G., &Lännergren, J., (2002). Muscle Fatigue: Lactic Acid or Inorganic Phosphate the Major Cause, News Physiol Sci. 17(17-21): 17-21

[73] Wei, D and Bovik, A. C. (1998). Generalized coiflets with nonzerocentered vanishing moments, IEEE Trans. on Circuits and Systems II. 45(8):988-1001

[74] Whipple,R.H., Wolfson,L.I., &Amerman,P.M., (1987). The relationship of knee and ankle weakness to falls in nursing home residents: an isokinetic study, J Am Geriatr Soc, 35(1):13-20

[75] Winter, D.A., (1995). Human balance and posture control during standing and walking, Gait Posture. 3(4):193–214

[76] Woollacott,M.H.,Shumway-Cook,A.,Nashner,L., (1986) Aging and posture control: changes in sensory organization and muscular coordination, Int J Aging Hum Dev. 23(2):97–114

Appendix A Calculate Mean Square Displacement

1. How to Calculate Mean Square Displacement Efficiently

Collins and De Luca (1994) proposed the following relation for COP.

$$\left\langle \Delta x^2 \right\rangle = 2D\Delta t$$

Simply, this equation indicated that there is a linear relation between the mean square displacement $\left\langle \Delta x^2 \right\rangle$ and time interval Δt. Unfortunately an explicit method to get the mean square displacement was not presented by the authors. Here, it is illustrated in more detail to ensure the correctness of diffusion algorithm implementation.

According to the definition of the mean square displacement

$$\left\langle \Delta r^2 \right\rangle = E\left(\left(x_i - x_{i+j}\right)^2\right)$$

It can be further written as

$$\left\langle \Delta r^2 \right\rangle = E\left(\left(x_i - x_{i+j}\right)^2\right) = E\left(x_i\right)^2 + E\left(x_{i+j}\right)^2 - 2E\left(x_i x_{i+j}\right)$$

The variance of sample is

$$Var\left(x_i\right) = E\left(\left(x_i - \overline{x_i}\right)^2\right) = E\left(x_i^2\right) - E^2\left(x_i\right)$$

The autocorrelation of sample is:

$$\rho_i = E\left(\left(x_i - \overline{x_i}\right)\left(x_{i+j} - \overline{x_{i+j}}\right)\right) = E\left(x_i\, x_{i+j}\right) - E\left(x_i\right)E\left(x_{i+j}\right) = E\left(x_i\, x_{i+j}\right) - E^2\left(x_i\right)$$

Therefore the mean square displacement was formulated as

$$\left\langle \Delta r^2 \right\rangle = Var(x_i) + Var(x_{i+j}) - 2\rho_i$$

, which can be further simplified to

$$\left\langle \Delta r^2 \right\rangle = 2Var(x_i) - 2\rho_i$$

Interestingly, this equation indicates that the mean square displacement is actually easy to calculate efficiently, and is equal to the difference between the variance and auto-correlation of COP data.

Matlab was chosen to implement the mean square displacement, the following codes being used for calculating the mean square displacement:

corrX = xcorr(tempX,tempX,'biased'); It is autocorrelation , where tempx is COP.

DetalR = 2*var(tempX) - 2.*corrX; it is mean square displacement, where DetalR is the mean square displacement.

2. More Detailed Power Spectrum and Local Maximum Lines Figures

To more clearly determine the details within COP data, using wavelet coefficients and the local maximum power spectrum wavelet transform, these plots were given in Figure A1. The corresponding relationship between the local maximum lines and the wavelet coefficients is given in Figure A2.

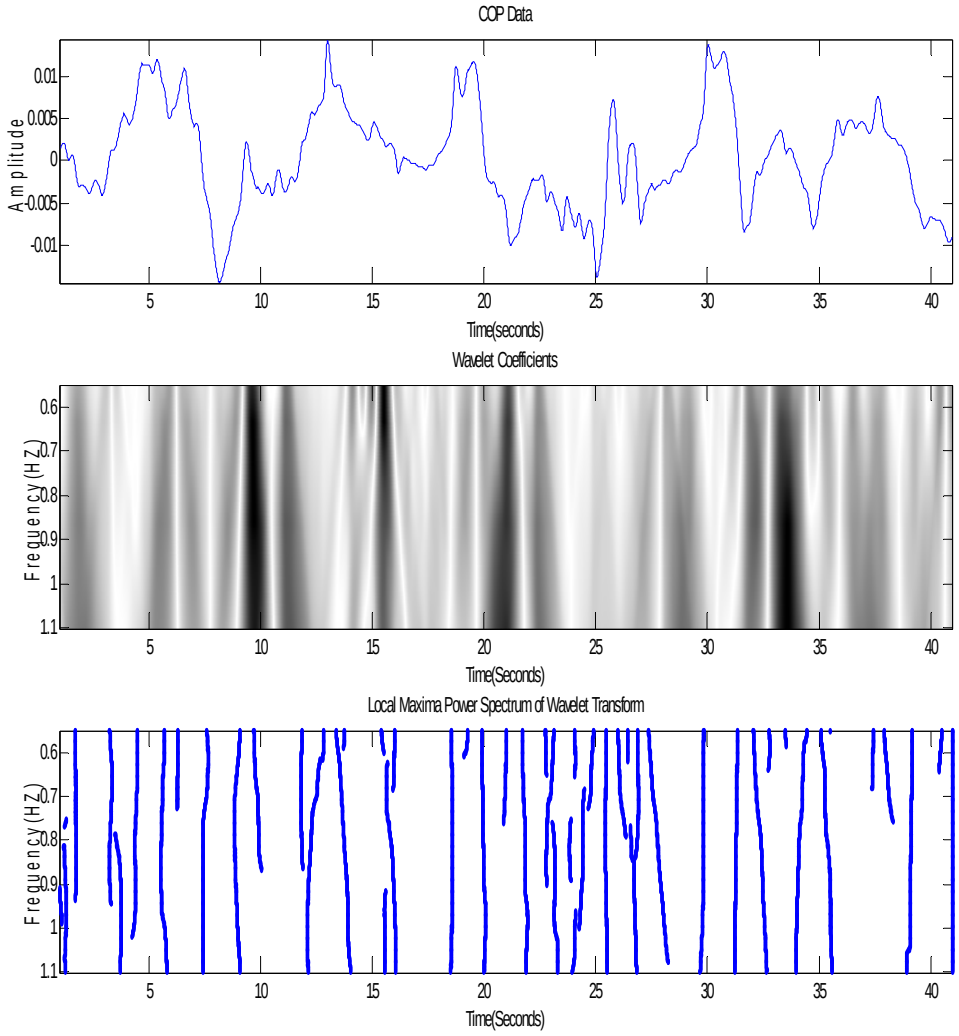

Figure A1 COP data, wavelet coefficients and local maximum power spectrum wavelet transform

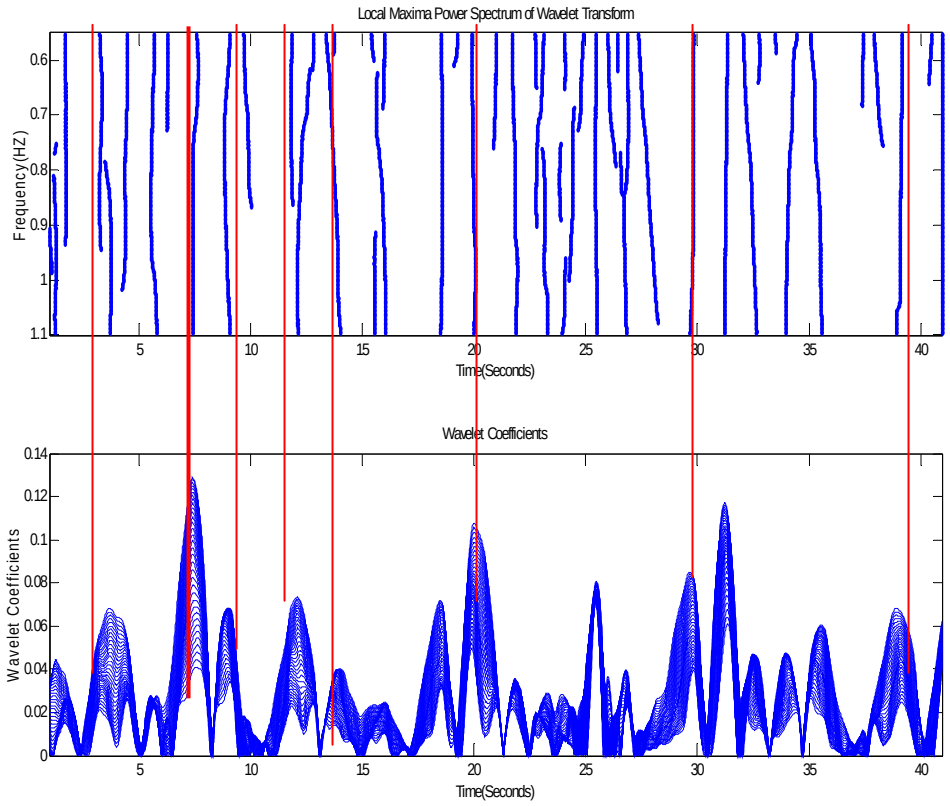

Figure A2 Local maximum power spectrum of wavelet transform and wavelet modules ($|Wavelet\ Coefficients|$, which is the $\sqrt{Power\,Spectrum}$)

Appendix B Results

Young Participants Diffusion Coefficients and Critical Time Interval from the Traditional Diffusion Algorithm (**bold, significant**)

	Fatigue Status	Ankle	Knee	Torso	Shoulder
ML Short-Term	**Pre-Fatigue**	2.09E-05 1.05E-05	2.11E-05 9.20E-06	**2.03E-05** **(1.58E-05)**	2.00E-05 1.41E-05
	Post-Fatigue	2.33E-05 9.75E-06	2.70E-05 1.16E-05	**3.85E-05** **(2.55E-05)**	2.59E-05 1.69E-05
ML Long-Term	**Pre-Fatigue**	5.57E-07 5.87E-07	6.35E-07 4.98E-07	4.15E-07 4.42E-07	3.66E-07 5.06E-07
	Post-Fatigue	1.19E-06 2.72E-06	7.67E-07 1.41E-06	1.05E-06 1.28E-06	9.24E-07 1.25E-06
AP Short-Term	**Pre-Fatigue**	3.72E-05 3.00E-05	3.43E-05 2.13E-05	3.95E-05 4.30E-05	3.99E-05 4.47E-05
	Post-Fatigue	4.01E-05 2.88E-05	4.53E-05 2.75E-05	5.96E-05 5.23E-05	4.29E-05 4.91E-05
AP Long-Term	**Pre-Fatigue**	5.77E-07 8.32E-07	5.53E-07 5. 89E-07	5.43E-07 5.64E-07	6.33E-07 9.32E-07
	Post-Fatigue	7.68E-07 6.69E-07	7.31E-07 1.28E-06	5.47E-07 7.77E-07	8.39E-07 1.74E-06

	Fatigue Status	Ankle	Knee	Torso	Shoulder
ML	**Pre-Fatigue**	1. 38(0. 39)	1.31(0.30)	1. 38(0. 33)	1. 45(0. 31)
	Post-Fatigue	1. 34 (0. 33)	1.38(0.29)	1.22(0.27)	1.49(0.26)
AP	**Pre-Fatigue**	1. 33 (0. 38)	1.33(0.27)	1.33(0.31)	1.46(0.39)
	Post-Fatigue	1. 31 (0. 27)	1.24(0.23)	1.30(0.26)	1.44(0.29)

Older Participants Diffusion Coefficients and Critical Time Interval from the Traditional Diffusion Algorithm

	Fatigue Status	Ankle	Knee	Torso	Shoulder
ML Short-Term	**Pre-Fatigue**	4.60E-05 4.07E-05	4.37E-05 4.53E-05	4.83E-05 6.57E-05	4.83E-05 4.26E-05
	Post-Fatigue	3.86E-05 3.01E-05	4.13E-05 4.07E-05	5.86E-05 7.15E-05	4.87E-05 5.57E-05
ML Long-Term	**Pre-Fatigue**	3.36E-07 3.16E-07	4.76E-07 5.47E-07	5.65E-07 1.20E-06	5.24E-07 6.14E-07
	Post-Fatigue	6.33E-07 4.78E-07	3.97E-07 3.47E-07	3.80E-07 3.97E-07	3.51E-07 2.17E-07
AP Short-Term	**Pre-Fatigue**	6.28E-05 5.66E-05	6.76E-05 6.16E-05	6.22E-05 5.82E-05	7.41E-05 8.01E-05
	Post-Fatigue	6.68E-05 5.54E-05	5.64E-05 5.73E-05	8.28E-05 1.12E-04	6.09E-05 5.43E-05
AP Long-Term	**Pre-Fatigue**	3.74E-07 4.41E-07	4.79E-07 7.92E-07	3.96E-07 4.12E-07	3.07E-07 3.09E-07
	Post-Fatigue	6.93E-07 6.00E-07	5.26E-07 6.17E-07	6.43E-07 6.14E-07	4.42E-07 4.01E-07

	Fatigue Status	Ankle	Knee	Torso	Shoulder
ML	**Pre-Fatigue**	1.13 (0.28)	1.18 (0.21)	1.22 (0.28)	1.13 (0.30)
	Post-Fatigue	1.27 (0.28)	1.30 (0.27)	1.19 (0.36)	1.33 (0.38)
AP	**Pre-Fatigue**	1.09 (0.24)	1.05 (0.25)	1.14 (0.24)	1.04 (0.20)
	Post-Fatigue	1.15 (0.25)	1.14 (0.18)	1.17 (0.37)	1.18 (0.26)

Young Participants Diffusion Coefficients and Critical Time Interval from the New Diffusion Algorithm (**bold, significant**)

	Fatigue Status	Ankle	Knee	Torso	Shoulder
ML Short-Term	**Pre-Fatigue**	1.62E-05 8.13E-06	1.70E-05 8.37E-06	**1.63E-05** **1.15E-05**	1.70E-05 9.98E-06
	Post-Fatigue	2.14E-05 1.01E-05	2.09E-05 8.41E-06	**3.25E-05** **2.15E-05**	2.04E-05 1.14E-05
ML Long-Term	**Pre-Fatigue**	2.30E-06 (gender) 2.25E-06	3.40E-06 (gender) 3.76E-06	**1.97E-06** **1.67E-06**	2.96E-06 (gender) 3.14E-06
	Post-Fatigue	3.01E-06 3.00E-06	3.43E-06 2.58E-06	**6.31E-06** **5.26E-06**	2.09E-06 2.30E-06
AP Short-Term	**Pre-Fatigue**	2.81E-05 1.90E-05	2.65E-05 1.31E-05	3.26E-05 (gender) 3.53E-05	3.23E-05 3.40E-05
	Post-Fatigue	3.72E-05 2.53E-05	3.19E-05 1.61E-05	4.65E-05 3.89E-05	3.64E-05 3.64E-05
AP Long-Term	**Pre-Fatigue**	1.96E-06 1.61E-06	2.16E-06 4.02E-06	2.53E-06 3.32E-06	2.06E-06 2.76E-06
	Post-Fatigue	3.03E-06 3.11E-06	2.28E-06 4.35E-06	1.09E-06 1.10E-06	2.61E-06 2.84E-06

	Fatigue Status	Ankle	Knee	Torso	Shoulder
ML	**Pre-Fatigue**	1.62 (0.29)	1.60 (0.23)	1.59 (0.18)	1.62 (0.23)
	Post-Fatigue	1.55 (0.14)	1.59 (0.27)	1.54 (0.16)	1.55 (0.16)
AP	**Pre-Fatigue**	1.49 (0.20)	1.51 (0.18)	1.45 (0.20)	1.47 (0.22)
	Post-Fatigue	1.43 (0.15)	1.55 (0.12)	1.44 (0.19)	1.47 (0.16)

Older Participants Diffusion Coefficients and Critical Time Interval from the New Diffusion Algorithm

	Fatigue Status	Ankle	Knee	Torso	Shoulder
ML Short-Term	**Pre-Fatigue**	3.63E-05 (gender) 3.72E-05	3.94E-05 (gender) 5.22E-05	3.85E-05 (gender) 6.04E-05	3.86E-05 (gender) 4.86E-05
	Post-Fatigue	3.33E-05 3.34E-05	3.11E-05 3.18E-05	5.19E-05 8.77E-05	3.70E-05 4.19E-05
ML Long-Term	**Pre-Fatigue**	4.05E-06 4.10E-06	4.36E-06 5.07E-06	3.33E-06 2.15E-06	4.83E-06 4.42E-06
	Post-Fatigue	4.96E-06 4.37E-06	3.31E-06 2.19E-06	5.10E-06 4.98E-06	2.98E-06 2.60E-06
AP Short-Term	**Pre-Fatigue**	5.31E-05 (gender) 5.01E-05	6.76E-05 (gender) 6.16E-05	5.08E-05 (gender) 4.93E-05	6.02E-05 (gender) 7.47E-05
	Post-Fatigue	5.96E-05 5.71E-05	5.10E-05 5.60E-05	7.83E-05 1.35E-04	5.97E-05 7.19E-05
AP Long-Term	**Pre-Fatigue**	3.08E-06 3.06E-06	3.74E-06 2.87E-06	3.23E-06 2.62E-06	2.66E-06 2.06E-06
	Post-Fatigue	3.03E-06 1.83E-06	2.48E-06 1.67E-06	3.28E-06 2.43E-06	2.13E-06 1.36E-06

	Fatigue Status	Ankle	Knee	Torso	Shoulder
ML	**Pre-Fatigue**	0.75 (0.07)	0.78 (0.09)	0.77 (0.09)	0.76 (0.09)
	Post-Fatigue	0.77 (0.08)	0.79 (0.10)	0.82 (0.13)	0.77 (0.06)
AP	**Pre-Fatigue**	0.73 (0.07)	0.72 (0.09)	0.72 (0.08)	0.72 (0.07)
	Post-Fatigue	0.74 (0.07)	0.74 (0.06)	0.77 (0.09)	0.76 (0.08)

Baseline Young Participants Diffusion Coefficients and Critical Time Interval from the New Diffusion Algorithm

	ECF	EOF	ECC	EOC	Romberg	One Leg
ML	1.54E-05	6.08E-06	5.02E-05	3.70E-05	3.70E-05	3.70E-05
Short-Term	8.09E-06	2.74E-06	8.88E-06	4.19E-05	4.19E-05	4.19E-05
ML	3.17E-06	2.94E-06	2.51E-06	2.98E-06	2.98E-06	2.98E-06
Long-Term	2.09E-06	1.65E-06	1.75E-06	2.60E-06	2.60E-06	2.60E-06
AP	2.59E-05	6.82E-06	7.19E-05	5.97E-05	5.97E-05	5.97E-05
Short-Term	1.39E-05	3.65E-06	1.54E-05	7.19E-05	7.19E-05	7.19E-05
AP	3.90E-06	9.19E-07	4.83E-06	2.13E-06	2.13E-06	2.13E-06
Long-Term	3.58E-06	8.38E-07	2.16E-06	1.36E-06	1.36E-06	1.36E-06

	ECF	EOF	ECC	EOC	Romberg	One Leg
ML	0.81	0.87	0.85	0.92	0.98	1.03
	0.06	0.09	0.07	0.13	0.65	0.46
AP	0.79	0.78	0.83	0.79	1.01	1.01
	0.09	0.08	0.09	0.07	0.55	0.47

Baseline Young Participants Diffusion Coefficients and Critical Time Interval from the Traditional Diffusion Algorithm

	ECF	EOF	ECC	EOC	Romberg	One Leg
ML Short-Term	1.15E-05 7.75E-06	4.32E-06 2.22E-06	1.50E-05 1.04E-05	5.48E-06 4.50E-06	3.70E-05 4.19E-05	3.70E-05 4.19E-05
ML Long-Term	1.87E-06 1.53E-06	2.09E-06 1.33E-06	1.62E-06 1.52E-06	2.49E-06 1.66E-06	2.98E-06 2.60E-06	2.98E-06 2.60E-06
AP Short-Term	1.84E-05 9.32E-06	4.40E-06 1.96E-06	2.50E-05 1.43E-05	6.37E-06 4.11E-06	5.97E-05 7.19E-05	5.97E-05 7.19E-05
AP Long-Term	1.68E-06 2.20E-06	5.60E-07 3.84E-07	8.59E-07 7.77E-07	5.22E-07 5.12E-07	2.13E-06 1.36E-06	2.13E-06 1.36E-06

	ECF	EOF	ECC	EOC	Romberg	One Leg
ML	1.27 0.54	1.08 0.40	1.17 0.50	1.09 0.55	1.20 0.43	0.97 0.46
AP	1.07 0.54	1.24 0.46	1.27 0.50	1.26 0.37	1.06 0.51	1.11 0.38

Baseline Older Participants Diffusion Coefficients and Critical Time Interval from the Traditional Diffusion Algorithm

	ECF	EOF	ECC	EOC	Romberg	One Leg
ML Short-Term	1.15E-05 7.75E-06	4.32E-06 2.22E-06	1.50E-05 1.04E-05	5.48E-06 4.50E-06	3.70E-05 4.19E-05	3.70E-05 4.19E-05
ML Long-Term	1.87E-06 1.53E-06	2.09E-06 1.33E-06	1.62E-06 1.52E-06	2.49E-06 1.66E-06	2.98E-06 2.60E-06	2.98E-06 2.60E-06
AP Short-Term	1.84E-05 9.32E-06	4.40E-06 1.96E-06	2.50E-05 1.43E-05	6.37E-06 4.11E-06	5.97E-05 7.19E-05	5.97E-05 7.19E-05
AP Long-Term	1.68E-06 2.20E-06	5.60E-07 3.84E-07	8.59E-07 7.77E-07	5.22E-07 5.12E-07	2.13E-06 1.36E-06	2.13E-06 1.36E-06

	ECF	EOF	ECC	EOC	Romberg	One Leg
ML	1.43 0.55	1.15 0.39	1.19 0.45	1.05 0.54	1.22 0.46	1.00 0.47
AP	1.05 0.58	1.14 0.46	1.29 0.53	1.38 0.39	0.97 0.56	1.08 0.36

Baseline Older Participants Diffusion Coefficients and Critical Time Interval from the New Diffusion Algorithm

	ECF	EOF	ECC	EOC	Romberg	One Leg
ML Short-Term	3.93E-05 3.97E-05	9.88E-06 3.90E-06	5.89E-05 7.05E-05	1.14E-05 7.57E-06	3.70E-05 4.19E-05	3.70E-05 4.19E-05
ML Long-Term	6.67E-06 6.55E-06	3.86E-06 2.91E-06	3.71E-06 2.53E-06	3.46E-06 2.45E-06	2.98E-06 2.60E-06	2.98E-06 2.60E-06
AP Short-Term	5.77E-05 4.73E-05	1.26E-05 7.31E-06	8.21E-05 5.75E-05	1.55E-05 9.35E-06	5.97E-05 7.19E-05	5.97E-05 7.19E-05
AP Long-Term	4.60E-06 3.30E-06	9.59E-07 5.67E-07	3.37E-06 2.63E-06	6.72E-07 5.89E-07	2.13E-06 1.36E-06	2.13E-06 1.36E-06

	ECF	EOF	ECC	EOC	Romberg	One Leg
ML	0.77 0.08	0.83 0.12	0.83 0.09	0.85 0.14	0.92 0.77	0.79 0.45
AP	0.74 0.08	0.71 0.07	0.78 0.09	0.73 0.06	0.84 0.47	0.78 0.43

Young Adult Short-Term Hurst Exponent

	Ankle	**Knee**	**Torso**	**Shoulder**
ML	0.9931 (pre-fatigue) 0.993087 (post-fatigue)	0.993027 (pre-fatigue) 0.992849 (post-fatigue)	0.993042 (pre-fatigue) 0.993338 (post-fatigue)	0.993184 (pre-fatigue) 0.993797 (post-fatigue)
AP	0.993471 (pre-fatigue) 0.993588 (post-fatigue)	0.993663 (pre-fatigue) 0.993577 (post-fatigue)	0.993755 (pre-fatigue) 0.993439 (post-fatigue)	0.993638 (pre-fatigue) 0.993188 (post-fatigue)

Appendix C IRB

VIRGINIA POLYTECHNIC INSTITUTE AND STATE UNIVERSITY

Informed Consent for Participants
In Research Projects Involving Human Subjects

Title of the Research Study
"Determining the relationships between different exercises and balance during static standing"

Investigators
Maury A. Nussbaum, Ph.D. 231-6053 – Department of Industrial and Systems Engineering
Michael L. Madigan, Ph.D. 231-1215 – Department of Engineering Science and Mechanics

I. Purpose of this Study
The purpose of this research study is to investigate the relationships between different exercises and balance during static standing. Falls from heights are a major problem in both industry and general society when measured in terms of human suffering and economic losses. Work tasks performed by various muscle groups may influence standing balance differently, and joints of the ankle, knee, lower torso, and shoulder are of particular interest due to their possible contributions to standing balance. Findings from this research study will provide a better understanding of the mechanisms associated with standing balance, and contribute to the development of practical interventions aimed at decreasing the risk of falls.

II. Procedures
A total of 40 adult participants will be used for the study.

The study will take place in either the Industrial Ergonomics and Biomechanics Lab (Department of Industrial and Systems Engineering) or the Musculoskeletal Biomechanics Lab (Department of Engineering Science and Mechanics). Upon arriving, you will be briefed of the study protocol, asked if you have any further questions, and asked to sign this informed consent form.

Prior to the experiment, several non-invasive position sensors will be placed on your body using double-sided tape. For this purpose, you will be required to wear a special clothing. The experimental session will be videotaped to help the investigators analyze your movement patterns during the experiment.

At the start of the experiment, you will be asked to stand still on a force platform for 75 seconds. You will then perform an exercise on a Biodex System (similar to a health club-type exercise apparatus) to work out muscles of your ankle, knee, lower torso, or shoulder.

Immediately following the exercise, you will return to the force platform for a second balance measurement. At this moment, balance measurements will be performed identically to the initial measurement procedure. This procedure will also be repeated every 5 minutes for 30 minutes to assess the recovery of balance following the exercise. The experiment is expected to take approximately 1.5 - 2 hours to complete.

In addition to an initial 1-hr practice session (which will also be used to obtain baseline measurements), you will be asked to complete the experiment in four separate occasions, once for each fatigue location (ankle, knee, lower torso, and shoulder). Each of these will be on different days separated by at least 48 hours.

III. Risks

The risks involved in this study are minimal. The overall physical exertion required during this experiment is not significantly larger than that required during common manual labor. You may feel residual muscle soreness, which will typically be gone within a few hours or within a day. If you experience any substantial amount of pain following an exercise, you should contact us immediately.

IV. Benefits

You will receive no direct benefit from participating in this study. The scientific community will benefit through the additional information that is expected to result from the completion of this study. This information will contribute to fall-related biomechanical knowledge that will be used to develop intervention techniques to prevent falls from heights.

No promise or guarantee of benefits has been made to encourage you to participate.

V. Extent of Anonymity and Confidentiality

The results of this research study may be presented at meetings or in publications. Your identity will not be disclosed in those presentations. All participants will be identified based only on their unique identifying number. Only the investigators and experimenters involved in the research will have access to these identifying numbers. The video recordings from this study will be analyzed and stored in the labs under the supervision of the investigators. Some photographs or video recordings may be shown to other scientists at the University or at scientific conferences.

VI. Compensation

You will be paid $10/hour for your participation in this study. A bonus in the amount of $20.00 will be provided at the completion of this study.

VII. Freedom to Withdraw

Your participation in this research study is voluntary. Refusal to participate will involve no penalty or loss of benefits to which you are otherwise entitled. You are free to withdraw from the study at any time without penalty.

VIII. Approval of Research

This research project has been approved, as required, by the Institutional Review Board for Research Involving Human Subjects at Virginia Polytechnic Institute and State University.

IRB Approval Date: 01/15/2005

Approval Expiration Date: 01/14/2006

IX. Participant Responsibilities

I voluntarily agree to participate in this study and to follow the responsibilities listed below:

a. To inform the investigator/experimenter as early as possible about a desire to discontinue participation in the study.
b. To inform the investigator of any medical conditions that might be adversely affected by the experiment, or those that might interfere with results of the experiment.

X. Participant's Permission

I have read and understand the Informed Consent and conditions of this project. I have had all my questions answered. I hereby acknowledge the above and give my voluntary consent:

_____	_____	_____
Signature	Printed name	Date
_____	_____	_____
Witness/experimenter	Printed name	Date

Should I have any pertinent questions about this research or its conduct, and research participants' rights, and whom to contact in the event of a research related injury to the participant, I may contact:

Principal Investigator:	Maury Nussbaum, PhD nussbaum@vt.edu	231-6053	
Co-Investigator:	Michael Madigan, PhD mlmadigan@vt.edu	231-1215	
Student Researcher:	Navrag Singh	231-1720	nbs@vt.edu
Chair, IRB:	David M. Moore, DVM moored@vt.edu	231-4991	

This Informed Consent is valid from 01/15/2005 to 01/14/2006.

Vita

Name: Hongbo Zhang

Birthday: 05.26.1974

Education:

BE, Jilin university, Automotive Engineering and Computer Engineering. 8.1994~8.1998

Master student, Virginia Tech, 8.2004~ present

Experience:

9.1998~2. 2000 Automation Institute of China Academy of Science, Beijing, working as a engineer for automatic control algorithm development and implementation. Successfully developing the client-server based real time control with the oracle database.

3.2000~12.2002 Tsinghua TongFang Corporation, working as a engineer for developing software for automatic biomedical image analysis, and oracle database.

1.2003~7.2004 Nanyang Technology university, Singapore, working as a research assistant for developing Intelligent transportation systems.

8.2004~ present Virginia Tech, working for the identification of the effects of human localized muscle fatigue on upright stance stability. It is a NIOSH supported project.

Research Interests:

Biomedical signal analysis, biomedical sensors development, human safety and health products development

Hobbies

Hiking, Playing Tennis, Swimming